

**REMOVAL OF MIXED VOCS OF BENZENE, TOLUENE AND XYLENE
BY A MULTISTAGE CORONA DISCHARGE SYSTEM**

Nitikorn Ditthawat

A Thesis Submitted in Partial Fulfilment of the Requirements
for the Degree of Master of Science
The Petroleum and Petrochemical College, Chulalongkorn University
in Academic Partnership with
The University of Michigan, The University of Oklahoma,
Case Western Reserve University, and Institut Français du Pétrole
2018

บทคัดย่อและแฟ้มข้อมูลฉบับเต็มของวิทยานิพนธ์ตั้งแต่ปีการศึกษา 2554 ที่ให้บริการในคลังปัญญาจุฬาฯ (CUIR)
เป็นแฟ้มข้อมูลของนิสิตเจ้าของวิทยานิพนธ์ที่ส่งผ่านทางบัณฑิตวิทยาลัย

The abstract and full text of theses from the academic year 2011 in Chulalongkorn University Intellectual Repository (CUIR)
are the thesis authors' files submitted through the Graduate School.

Thesis Title: Removal of Mixed VOCs of Benzene, Toluene and Xylene
by a Multistage Corona Discharge System
By: Nitikorn Ditthawat
Program: Petroleum Technology
Thesis Advisor: Prof. Sumaeth Chavadej

Accepted by The Petroleum and Petrochemical College, Chulalongkorn University, in partial fulfilment of the requirements for the Degree of Master of Science.

..... College Dean
(Prof. Suwabun Chirachanchai)

Thesis Committee:

.....
(Prof. Sumaeth Chavadej)

.....
(Assoc. Prof. Boonyarach Kitiyanan)

.....
(Assoc. Prof. Vissanu Meeyoo)

ABSTRACT

5973010063: Petroleum Technology Program

Nitikorn Ditthawat: Removal of Mixed VOCs of Benzene, Toluene
and Xylene by a Multistage Corona Discharge System

Thesis Advisor: Prof. Sumaeth Chavadej 72 pp.

Keywords: Corona discharge/ Plasma

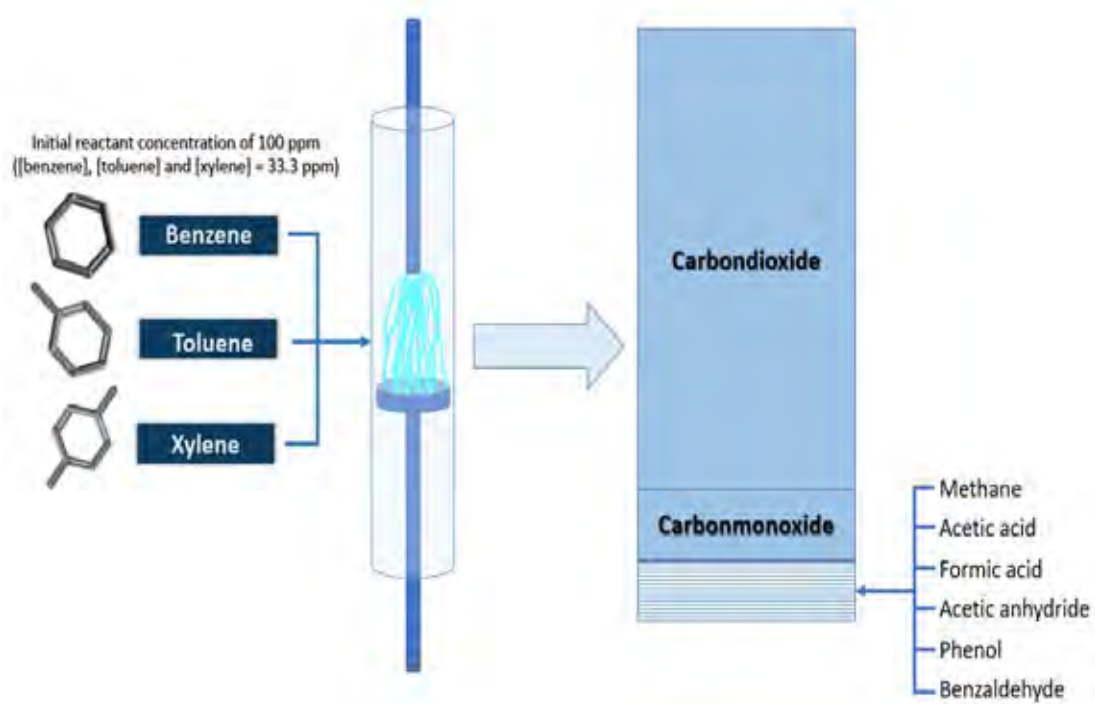
The oxidation of mixed volatile organic compounds (VOCs) of benzene, toluene and xylene in non-thermal plasma corona discharge was investigated. An initial total VOCs concentration of 100 ppm and feed flow rate of 50.0 ml/min were firstly fixed to investigate the effects of an applied voltage and input frequency on VOCs conversion, power consumption and CO₂ and CO selectivities. For a single stage plasma system, under the optimum applied voltage of 8 kV and input frequency of 500 Hz, the system gave the high CO₂ selectivity with the low CO selectivity and the lowest power consumption. At the optimum operationable conditions, the effect of reactant feed flow rate and stage number were examined. The increase in reactant feed flow rate from 25 to 125 ml/min corresponding to the reduction of residence time from 0.92 to 0.19 s resulted in decreases in both of VOCs conversion and CO₂ selectivity from 97.7 to 63.9% and 84.0 to 22.6%, respectively while the CO selectivity was increased from 8.2 to 62.4%. An increase in stage number from one to two stages caused an increase in the total VOCs conversion approximately 100% especially for the feed flow rate of 100 ml/min.

บทคัดย่อ

นิพนธ์ ดิษฐวัฒน์ : การสลายตัวของเบนซีนโทลูอินและไซลีนในเครื่องปฏิกรณ์พลาสมาแบบปล่อยโคโรนาชนิดอนุกรมที่อุณหภูมิห้องและความดันบรรยากาศ (Removal of Mixed VOCs by a Multistage Corona Discharge System) อ. ที่ปรึกษา ศ. ดร. สุเมธ ชวเดช 72 หน้า

ในงานวิจัยนี้ เป็นการศึกษาการสลายตัวของสารประกอบอินทรีย์ชนิดระเหยง่ายซึ่งประกอบไปด้วย เบนซีน โทลูอิน และไซลีนในเครื่องปฏิกรณ์พลาสมาแบบปล่อยโคโรนาซึ่งต่อแบบอนุกรมจำนวนสี่เครื่อง ที่อุณหภูมิห้องและความดันบรรยากาศ เพื่อหาสถานะที่เหมาะสมสำหรับการสลายสารประกอบอินทรีย์ชนิดระเหยง่าย โดยทำการปรับปัจจัยต่างๆที่ส่งผลต่อการสลายตัวของสารประกอบอินทรีย์ชนิดระเหยง่าย ได้แก่ แรงดันไฟฟ้า ความถี่ ระยะเวลาที่สารเกิดปฏิกิริยา และจำนวนของเครื่องปฏิกรณ์ ผลการทดลองพบว่าสถานะที่เหมาะสมสำหรับเครื่องปฏิกรณ์พลาสมาแบบปล่อยโคโรนาจำนวนหนึ่งเครื่อง ได้แก่ แรงดันไฟฟ้า 8 กิโลโวลต์ ความถี่ 500 เฮิร์ต ที่อัตราการไหลของอากาศ 50 มิลลิลิตรต่อนาที ซึ่งให้ค่าการสลายสารประกอบอินทรีย์ชนิดระเหยง่ายร้อยละ 94 และค่าการเลือกเกิดแก๊สคาร์บอนไดออกไซด์และแก๊สคาร์บอนมอนอกไซด์ร้อยละ 80 และ 11 ตามลำดับ เมื่อศึกษาผลของอัตราการไหลของอากาศหรือระยะเวลาในการเกิดปฏิกิริยาพบว่า อัตราการไหลของอากาศส่งผลต่อค่าการสลายสารประกอบอินทรีย์ชนิดระเหยง่าย ค่าการเลือกเกิดแก๊สคาร์บอนไดออกไซด์และคาร์บอนมอนอกไซด์ โดยค่าการสลายตัวสารประกอบอินทรีย์ชนิดระเหยง่ายและค่าการเลือกเกิดแก๊สคาร์บอนไดออกไซด์มีค่าลดลง เมื่ออัตราการไหลของอากาศเพิ่มขึ้นจาก 50 เป็น 125 มิลลิลิตรต่อนาที ในขณะที่ค่าการเลือกเกิดแก๊สคาร์บอนมอนอกไซด์มีค่าเพิ่มขึ้น เมื่อศึกษาผลของจำนวนเครื่องปฏิกรณ์พลาสมาแบบปล่อยโคโรนาพบว่า สารประกอบอินทรีย์ชนิดระเหยง่ายสลายตัวคิดเป็นร้อยละ 100 เมื่อไหลผ่านเครื่องปฏิกรณ์พลาสมาแบบปล่อยโคโรนาจำนวนสองเครื่อง และค่าการเลือกเกิดแก๊สคาร์บอนไดออกไซด์และคาร์บอนมอนอกไซด์จะไม่เปลี่ยนแปลงเมื่อไหลผ่านเครื่องปฏิกรณ์ตั้งแต่สามเครื่องเป็นต้นไป โดยจะมีค่าการเลือกเกิดคาร์บอนไดออกไซด์และคาร์บอนมอนอกไซด์ร้อยละ 76 และร้อยละ 17 ตามลำดับ

GRAPHICAL ABSTRACT



The oxidation reaction of mixed VOCs of benzene, toluene and xylene by corona discharge reactor.

ACKNOWLEDGEMENTS

This research has been successful by the valuable contribution and assistance of the following persons and organizations:

Foremost, I am heartily grateful to my advisors, Prof. Sumaeth Chavadej, whose expertise, generous guidance and encouragement from repairing line operation until the completely finishing. During the journey to my M.S. graduation, I have gained great knowledge together with precious experiences, which could enhance my performance in research work.

This thesis work is funded by the Petroleum and Petrochemical College; and the National Center of Excellence for Petroleum, Petrochemicals, and Advanced Materials, Thailand.

I deeply appreciate all of the Petroleum and Petrochemical College's staffs for their assistance in many aspects regarding restoration of the experimental instrument and electrical parts even instructive information for characterization equipment.

Finally, I would like to express my sincere thanks to all of my PPC friends for their friendly support throughout the period of this research. Last but not the least, I am greatly indebted to my parents and my family for their love and understanding.

TABLE OF CONTENTS

	PAGE
Title Page	i
Abstract (in English)	iii
Abstract (in Thai)	iv
Acknowledgements	v
Table of Contents	vi
List of Tables	x
List of Figures	xi
 CHAPTER	
I INTRODUCTION	1
 II THEORETICAL BACKGROUND AND LITERATURE REVIEW	
2.1 Benzene	3
2.1.1 Common Characteristics	3
2.1.2 Manufacturing	4
2.1.3 Uses	4
2.1.4 Benzene Toxicity	4
2.2 Toluene	6
2.2.1 Common Characteristics	6
2.2.2 Manufacturing	7
2.2.3 Uses	7
2.2.4 Toluene Toxicity	7
2.3 Xylene	8
2.3.1 Common Characteristics	8
2.3.2 Manufacturing	9

CHAPTER	PAGE
2.3.3 Uses	10
2.3.4 Xylene Toxicity	10
2.4 Typical Exposure Situation of VOCs	11
2.5 Control of VOCs	12
2.5.1 Common VOCs Removal Methods	12
2.5.2 Bio-Treatment	13
2.6 Plasma	14
2.6.1 Plasma Definition	14
2.6.2 Plasma Generation	14
2.6.3 Collision Processes in Plasma	15
2.6.3.1 Excitation	16
2.6.3.2 Ionization	16
2.6.3.3 Dissociation	16
2.6.3.4 Electron Attachment	16
2.6.4 Plasma Classification	17
2.6.5 Corona Discharge Process	17
2.6.6 Gliding Arc Discharges	19
2.6.7 Dielectric Barrier Discharges	22
III EXPERIMENTAL	34
3.1 Materials	34
3.2 Experiment Setup	34
3.2.1 Feed Reactant and Carried Gas Section	35
3.2.2 Reactor Section	36
3.2.3 Power Supply Section	36

CHAPTER	PAGE
3.2.4 Analytical Section	37
3.3 Experimental Procedure	48
3.4 Reaction Performance Evaluation	39
IV RESULTS AND DISCUSSION	41
4.1 Condensed Products Analysis	41
4.2 Effect of Applied Voltage	43
4.2.1 The Effect of Applied Voltage on Reactant Conversion	43
4.2.2 The Effect of Applied Voltage on CO and CO ₂ selectivity	46
4.2.3 The Effect of Applied Voltage on Power Consumption	47
4.3 The Effect of Input Frequency	48
4.3.1 The Effect of Input Frequency on Reactant Conversion	49
4.3.2 The Effect of Input Frequency on CO and CO ₂ Selectivity	51
4.3.3 The Effect of Input Frequency on Power Consumption	52
4.4 The effect of Feed Flow Rate	53
4.4.1 The Effect of Reactant Feed Flow Rate on Reactant Conversion	54
4.4.2 The Effect of Reactant Feed Flow Rate on CO and CO ₂ Selectivity	55

CHAPTER	PAGE
4.4.3 The Effect of Reactant Feed Flow Rate on Power Consumption	56
4.5 Effect of Stage Number	57
4.5.1 The Effect of Stage Number on Reactant Conversion	57
4.5.2 The Effect of Stage Number on CO and CO ₂ Selectivity	59
4.5.3 The Effect of Stage Number on Power Consumption	60
4.6 Effect of Stage Number by Fixing the Residence Time	61
4.6.1 Effect of Stage Number at Residence Time on VOCs Conversion	61
4.6.2 Effect of Stage Number at Residence Time CO and CO ₂ Selectivity	62
V CONCLUSIONS AND RECOMMENDATIONS	64
5.1 Conclusions	64
5.2 Recommendations	65
REFERENCES	66
APPENDIXS	67
Appendix A Experimental Data	67
Appendix B Products Information from GC-MS Analysis	71
CURRICULUM VITAE	72

LIST OF TABLES

TABLE		PAGE
2.1	Physical properties of benzene	3
2.2	Physicals properties of toluene	6
2.3	Physicals properties of xylene	9
A1	Effect of applied voltage on VOCs conversion and CO and CO ₂ selectivity of the studied input frequency of 300, 400, 500 and 600 Hz, an initial concentration of 100 ppm, total feed flow rate of 50.0 ml/min and electrode gap distance of 10 mm.	67
A2	Effect of input frequency on VOCs conversion and CO and CO ₂ selectivity of the studied applied voltage of 4, 6, 8 and 10 kV, an initial concentration of 100 ppm, total feed flow rate of 50.0 ml/min and electrode gap distance of 10 mm.	68
A3	Effect of reactant feed flow rate on VOCs conversion and CO and CO ₂ selectivity at applied voltage of 8 kV, input frequency of 500 Hz, an initial concentration of 100 ppm and electrode gap distance of 10 mm.	69
A4	Effect of stage number on VOCs conversion and CO and CO ₂ selectivity at applied voltage of 8 kV, input frequency of 500 Hz, an initial concentration of 100 ppm, electrode gap distance of 10 mm and reactant feed flow rate of 50.0 and 100.0 ml/min.	70
B1	Products information from GC-MS analysis	71

LIST OF FIGURES

FIGURE	PAGE
2.1	Chemical structure of benzene. 4
2.2	Chemical structure of toluene. 6
2.3	Chemical structure of xylene. 9
2.4	Ambient Air Concentrations of BTEX and CCs. 11
2.5	Collision Processes in a Plasma. 15
2.6	The Configuration of Positive and Negative Corona Discharge. 18
2.7	Start, Life and Disappearance of the Gliding Discharges. 20
2.8	Voltage, Current and Power Curves. 21
2.9	Historic Ozone Discharge Tube of W.Siemens. 22
2.10	Basic Dielectric-Barrier Discharge Configurations. 23
2.11	Total VOC Removal as a Function of Inlet Toluene Concentration. 24
2.12	Effect of Specific Input Energy to Toluene Removal Efficiency and Ozone Concentration. 25
2.13	Effect of Frequency on Benzene Conversion at Different Stage Numbers. 26
2.14	Effect of Applied Voltage on Benzene Conversion at Different Stage Numbers. 27
2.15	Effect of Feed Flow Rate on Benzene conversion at Different Stage Numbers. 27
2.16	Effects of Discharge Polarity on Formaldehyde Conversion. 28
2.17	Effects of Discharge Tooth Wheel-Interval on Energy Input and Formaldehyde conversion. 29
2.18	Effects of Ddischarge Tooth Wheel-Number on Energy Input and Formaldehyde Conversion. 30

FIGURE		PAGE
2.19	Effects of Downstream Catalyst on Formaldehyde Conversion and O ₃ Outlet Concentration.	30
2.20	Possible Path Way for p-Xylene-OH Destruction.	33
3.1	Experimental Setup by Using Corona Discharge Reactors.	35
3.2	Configuration of Corona Discharge Reactor.	36
3.3	Schematic of the Power Supply Unit.	37
4.1	Chromatogram of GC–MS Analysis for Mixed VOCs Degradation Products.	42
4.2	Summary of Products of the Studied Mixed VOCs Oxidation by Corona Discharge.	42
4.3	Effect of Applied Voltage on VOCs Conversion.	44
4.4	Effect of Applied voltage on measured current across electrodes.	44
4.5	Effect of input frequency on VOCs, benzene, toluene and xylene conversion at optimum applied voltage.	45
4.6	Effect of applied voltage on CO ₂ and CO selectivity.	47
4.7	Effect of applied voltage on power consumption.	48
4.8	Effect of input frequency on VOCs conversion.	49
4.9	Effect of input frequency on measured current across electrodes.	50
4.10	Effect of applied voltage on VOCs, benzene, toluene and xylene conversion at optimum input frequency.	50
4.11	Effect of input frequency on CO ₂ and CO selectivity.	52
4.12	Effect of input frequency on power consumption.	53
4.13	Effect of reactant feed flow rate on VOCs, benzene, toluene and xylene conversion at optimum applied voltage.	54
4.14	Effect of reactant feed flow rate on CO ₂ and CO selectivity.	55
4.15	Effect of reactant feed flow rate on power consumption.	56

FIGURE		PAGE
4.16	Effect of stage number on VOCs conversion.	58
4.17	Effect of stage number on VOCs, benzene, toluene and xylene conversion at optimum reactant feed flow rate.	58
4.18	Effect of stage number on CO ₂ and CO selectivity.	59
4.19	Effect of stage number on power consumption.	60
4.20	Effect of residence time at 0.46 on VOCs, benzene, toluene and xylene conversion.	62
4.21	Effect of residence time at 0.46 on CO ₂ and CO selectivity.	63

CHAPTER I

INTRODUCTION

Nowadays, number of automobile such as car is continuously increase around the world. So, the fuel consumption rate also increases. The direct result is there are more exhaust gas form those automobiles and from the outlet gas steam a refinery. Gas emits from automobile are NO_x , SO_x , H_2S and mainly volatile organic compounds (VOCs). Because of high volatility, VOCs spread in atmosphere rapidly. Furthermore, VOCs has large negative impact to both environment and human health such as ozone network depletion and Carcinogenic for human (Vandenbroucke *et al.*, 2009).

Volatile Organic Compounds (VOCs) is substance which main element are organic hydrogen and carbon. It can be liquid or solid at ambient condition but its evaporation rate to atmosphere is high (Chavadej *et al.*, 2007). Benzene, Toluene and Xylene are used widely in downstream petrochemicals plant as feedstock. In addition, they can be used directly as solvent (Elfadly *et al.*, 2016).

There are many conventional methods to control the emission of VOCs in air such as adsorption, membrane separation, bio- reaction, catalytic and thermal oxidation. By the way, those methods have a lot of disadvantages such as efficiency of system, operation hardness and cost efficiency (Vandenbroucke *et al.*, 2009).

Non-thermal plasma is one of methods that has a lot of advantages among the rest methods because of high removal efficiency and low energy consumption. Non-thermal plasma removes VOCs by generating a lot of active chemicals species to react with VOCs which is toxic species then VOCs become to non- toxic species. Furthermore, size of non- thermal plasma is more compact than another removal method (Ondarts *et al.*, 2017). Consequently, it very important to remove VOCs from air before it will be exhaust from any system to reduce effect of those chemical species to both environment and human. There are so many type of non-thermal plasma which are glow discharge, dielectric barrier or silent discharge, microwave discharge, radio frequency discharge, gliding arc discharge and corona discharge.

For corona discharge, plasma is generated by increasing voltage between two sides of electrode (pin and plate side) until electron jump from one side of electrode to another side (Feng *et al.*, 2013). Because of short reaction time in the corona discharge reactor, there is some limitation of removal efficiency. So, removal efficiency will be increase if the number of reactor increase (Chavadej *et al.*, 2007).

In the present work, the multi stages corona discharge reactors will be used to investigate the plasma oxidation of mixed VOCs which is mixture of benzene, toluene and xylene. The operating parameter are applied voltage, input frequency, reactant feed flow rate and stage number.

CHAPTER II

THEORETICAL BACKGROUND AND LITERATURE REVIEW

Volatile organic compounds (VOCs) are organic hydrocarbon that evaporate at normal temperature (293.15 K) and pressure (101.325 kPa) to atmosphere rapidly. The main composition of VOCs are benzene toluene and xylene. Each of them has individual toxicity depend on its concentration and emission sources. They have been used in petrochemical plant, paint, lacquers and leather tanning process (Kamal *et al.*, 2016).

2.1 Benzene

2.1.1 Common Characteristic

Benzene is organic aromatic hydrocarbon which formula C_6H_6 . It found naturally in crude oil and it is used widely in petrochemicals plants. Benzene is a colorless and highly flammable liquid. In addition, benzene is used in octane booster application for gasoline. The physicals properties of benzene are shown in table 2.1.

Table 2.1 Physicals properties of benzene

Properties	
Chemical formula	C_6H_6
Molar mass	78.11 g/mol
Appearance	Colorless liquid
Odor	Aromatic, Gasoline-like
Density	0.8765 g/cm^3 (at 20°C)
Melting point	5.53 °C
Boiling point	80.1 °C
Vapor pressure	12.7 kPa (at 25°C)

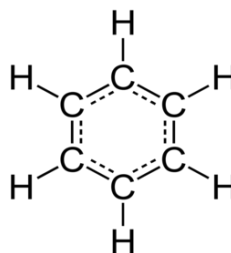


Figure 2.1 Chemical structure of benzene

2.1.2 Manufacturing

Benzene is generally used as solvent and petrochemical feedstock. It has been produced by applying some chemical process such as catalytic reforming, steam cracking toluene hydrodealkylation and toluene disproportionation.

2.1.3 Uses

Benzene is typically used as intermediate for other chemicals such as cumene, cyclohexane, nitrobenzene, alkylbenzene and mainly ethylbenzene. Half of produced benzene is used for ethylbenzene production because it is a precursor for styrene which is used to make polystyrene. Another 20% is for cumene production which is a phenol intermediate. Furthermore, it can be used directly as solvent and gasoline additive.

2.1.4 Benzene toxicity

There are many main factors that need to be concerned before people will be harmed by benzene, which are dosage (how much), duration (how long) and how benzene interacts with the body. Benzene concentration ranges from 0.02 to 34 parts of benzene in a billion parts of air (ppb). People will smell benzene if there are approximately 60 parts of benzene in a million parts of air (ppm). Normally, people in cities or industrial areas will be exposed to higher benzene concentrations than people in the countryside. Furthermore, drinking water typically contains less than 0.1 ppb.

Benzene can enter the body by many ways such as breathing, gastrointestinal tract and directly through the skin. It will spread in the body by the blood system and then it will temporarily store in bone marrow and fat.

For short time exposure (5-10 minutes), at extremely high concentration of benzene in air (10,000-20,000 ppm) can cause of death. At lower level (700-3,000 ppm) can cause of rapid heart rate, headaches, confusion and unconsciousness. For food contamination, benzene can cause of irritation, convulsions and vomiting.

Moreover, benzene causes of blood tissue especially bone marrow problem for people who breath it for long time. These effects can disturb blood production and a decrease in important blood component.

For long time exposure, benzene can cause of blood-forming organ cancers or leukemia. Both of International Agency for Cancer Research and the Environmental Protection Agency (EPA) have determined that benzene is carcinogenic to humans. In addition, it can cause of the reproductive organs. In case of woman worker at high concentration of benzene, their mouth has irregular shape and decrease size of ovaries. However, the exact concentration of benzene is unknown. For pregnant animals, benzene can cause of non-development of embryo, reducing of birth weight and bone marrow damage.

Many governments have developed the regulations and recommendations to protect public health and they are enforced by law. The EPA, the Occupational Safety and Health Administration (OSHA) and the Food and Drug Administration (FDA) are example of agencies that develop the regulations for toxic substances. Recommendations and regulations are expressed as “not-to-exceed” level. For benzene, EPA has set the maximum limit at 5 ppb and they found that 10 ppb of benzene in air can cause of cancer in human. Furthermore, the maximum for short term exposed (less than 10 days) is 200 ppb for children.

2.2 Toluene

2.2.1 Common characteristic

Toluene is colorless and water insoluble liquid. It is mono substituted of benzene by methyl group. As such, it's IUPAC systemic name is methylbenzene. It is widely used as feedstock and solvent. The physicals properties of toluene are shown in table 2.2.

Table 2.2 Physicals properties of toluene

Properties	
Chemical formula	C ₇ H ₈
Molar mass	92.14 g/mol
Appearance	Colorless liquid
Odor	Sweet, pugent, benzene-like
Density	0.87 g/cm ³ (at 20°C)
Melting point	-95 °C
Boiling point	111 °C
Vapor pressure	2.8 kPa (at 20°C)

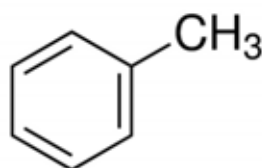


Figure 2.2 Chemical structure of toluene

2.2.2 Manufacturing

Toluene is by product of gasoline production by catalytic reforming or ethylene cracking process and it is found naturally at low level in crude oil. For laboratory preparation, it is prepared by chemical reaction between benzene and methyl chloride in present of Lewis acid such as aluminium chloride.

2.2.3 Uses

Toluene is used as precursor for benzene production by hydrodealkylation and for benzene and xylene production by disproportionation. In addition, it can be use directly as solvent for paints, paint thinners, silicone sealants and adhesives. For fuel application, it can be used as octane booster for gasoline.

2.2.4 Toluene toxicity

Toluene is colorless liquid with distinctive smell. It can be use as solvent, feedstock for petrochemical plants and octane booster for gasoline. Toluene is naturally found in crude oil.

Toluene can be released into the air, water, and soil at places where it is produced or used. Toluene is commonly found in air, particularly when there is heavy vehicular traffic. Toluene is present at average level about 1-35 parts per billion by volume (ppbv) in outdoor air at United States. In the other hand, the average amount of toluene in indoor air is higher than out door depend on place because of using paint thinners and tobacco products.

Toluene can contaminate with water and ground water by leaking of petroleum products and gasoline. When that water come out to surface toluene will evaporate rapidly to atmosphere. In addition, toluene which is used in paint also can evaporate to atmosphere.

Toluene enter to human body by breathing or eating the contaminate air or water. However, the case that toluene contaminate with drinking water is found not pretty much. But for air contamination is frequently found due to evaporation. Toluene can go to human organs by blood system after breathing the contaminate air. As the same way, toluene will spread in body if it enters to human body by eating. Little amount of toluene will accumulate in tissue and the less will be removed from body.

The accumulated toluene will be eliminated from body by changing in to the less harmful chemical species.

For short period exposure, it will cause headaches and sleepiness. However, the effect depends on amount, period, genetic susceptibility and age. The most dangerous activity is exposure in large amount in a short time. At first, you will feel light-headed. If exposure continues, you can become dizzy, sleepy, or unconscious, and you might even die. Toluene causes death by interfering with the way you breathe and the way your heart beats. When exposure is stopped, the sleepiness and dizziness will go away and you will feel normal again.

For moderate period exposure, it will cause of confusion, weakness, memory loss and loss of appetite. These symptoms usually disappear when exposure is stopped. Combinations of toluene and some common medicines like aspirin and acetaminophen may increase the effects of toluene on your hearing. For long period exposure, toluene can permanently damage brain system which is cause of speech, vision, muscle control and balance problem

However, The International Agency for Research on Cancer, The U.S. EPA, The American Conference of Governmental Industrial Hygienists and The U.S. National Toxicology Program have determined that toluene is not classifiable as to its carcinogenicity in humans.

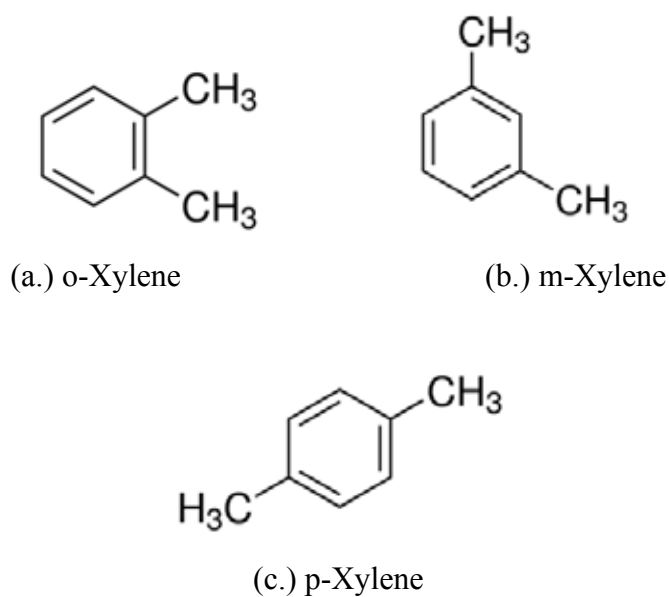
2.3 Xylene

2.3.1 Common characteristic

Xylene or dimethyl benzene is one of three isomers of dimethylbenzene or a mixed of any isomer. Chemical formula is $(\text{CH}_3)_2\text{C}_6\text{H}_4$. Every isomer has benzene in central of molecule and substituted by two methyl groups. They are all colorless, flammable liquids, some of which are of great industrial value.

Table 2.3 Physicals properties of xylene

Properties	Isomer		
	o-Xylene	m-Xylene	p-Xylene
Chemical formula	C ₈ H ₁₀		
Molar mass	106.16 g/mol		
Appearance	Clear and Colorless liquid		
Density	0.88 g/mL, liquid	0.86 g/ml, liquid	0.86 g/mL, liquid
Melting point	-25 °C	-48 °C	13 °C
Boiling point	144 °C	139 °C	138 °C

**Figure 2.3** Chemical structure of xylene (a.) o-Xylene, (b.) m-Xylene and (c.) p-Xylene

2.3.2 Manufacturing

Xylenes are produced in industries by methylation of toluene and benzene. Commercial or laboratory grade xylene produced usually contains about 40-65% of m-xylene and up to 20% each of o-xylene, p-xylene and ethylbenzene. The ratio of isomers can be shifted to favor the highly-valued p-xylene via the patented

UOP-Isomar process or by trans alkylation of xylene with itself or trimethylbenzene. These conversions are catalyzed by zeolites. ZSM- 5 is used to facilitate some isomerization reactions leading to mass production of modern plastics.

2.3.3 Uses

In polymer industries point of view, p-xylene is used for terephthalic acid and dimethyl terephthalate production which are used as monomer for polyethylene terephthalate (PET) production. PET is widely used for plastic and clothing. p-Xylene production is more than half of all xylene production and 98% of p-xylene has been used in this application. For other uses, xylene has been used as solvent in form of mixed isomer with small amount of ethylbenzene and in printing, rubber and leather industries.

2.3.4 Xylene toxicity

Main sources of xylene emission are industrial, automobile exhaust and laboratory solvent. The average level of xylene in United States at outdoor air is 1-30 parts of xylene in billion parts of air (ppb) and indoor air is 1-10 ppb. However, xylene is not commonly found in drinking water which is less than 2 ppb. Xylenes enter to human body by breathing or eating a contaminated air or food and they are absorbed rapidly through lungs and gut. For liquid xylenes, they are also absorbed easily through skin.

In people and laboratory animals, xylene is chemically changed, primarily in the liver, into a different form that is more water soluble and is rapidly removed from the body in urine. Some unchanged xylene also leaves in the breath from the lungs within a few seconds after xylene is absorbed.

Short-term exposure of people to high levels of xylene can cause irritation of the skin, eyes, nose, and throat. Both short- and long-term exposure to high concentrations of xylene can also cause a number of effects on the nervous system, such as headaches, lack of muscle coordination, dizziness, confusion, and changes in one's sense of balance. Some people exposed to very high levels of xylene for a short period of time have died.

2.4 Typical Exposure Situation of VOCs

Navaporn *et al.* (2017) investigated the level of volatiles organic compounds (VOCs) which are benzene, toluene, ethylbenzene and xylenes (BTEX) and carbonyl compounds (CCs) at inner city of Bangkok, Thailand. BTEX and CCs are toxic air pollutants including carcinogenic compounds that have high potential to cause health problems. According to the EPA's cancer classifications, benzene is classified as a human carcinogen, and formaldehyde, ethylbenzene and acetaldehyde are probable human carcinogens. High traffic density leads to higher levels of air pollution and roadside workers who are exposed to these pollutants everyday are therefore at risk.

The studied locations are around the Pathunwan district which are Pathumwan intersection (PT), Chaloe Pao junction (CP), Sam Yan intersection (SY) and Henry Dunant intersection (HD). Researchers found that the highest concentration of BTEX was detected at HD (range from 1570.46 to 5553.77 $\mu\text{g}/\text{m}^3$, average 2968.96 $\mu\text{g}/\text{m}^3$) and the lowest at SY (range from 1179.99 to 2859.31 $\mu\text{g}/\text{m}^3$, average 1964.52 $\mu\text{g}/\text{m}^3$). For CCs compounds, formaldehyde and acetaldehyde were found at the most abundant in CCs. Similar to BTEX, the highest average concentrations of both formaldehyde and acetaldehyde were detected at HD (range from 13.76 to 32.42 $\mu\text{g}/\text{m}^3$, average, 21.50 $\mu\text{g}/\text{m}^3$, and range from 3.90 to 99.70 $\mu\text{g}/\text{m}^3$, average, 64.82 $\mu\text{g}/\text{m}^3$, respectively).

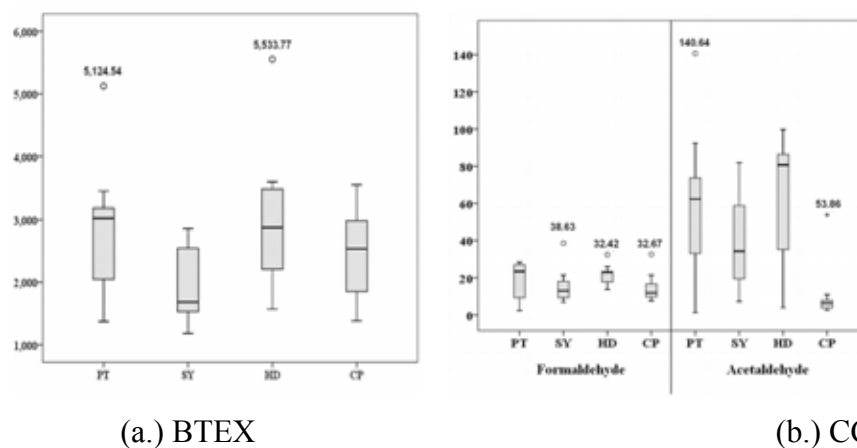


Figure 2.4 Ambient air concentrations of (a.) BTEX and (b.) CCs for 48 sampling sites.

2.5 Control of VOCs

Volatile Organic Compound (VOCs) are man-made naturally occurring highly reactive hydrocarbons. VOCs is any organic compound which boiling point from (50-100 °C) to (240-260 °C) and its vapor pressure more than 102 kPa at 25°C. Most of VOCs are toxic to animals and humans. Aydin *et al.* (2012) review the removal method by following.

2.5.1 Common VOCs Removal Methods

For liquid phase removal, adsorption by activated carbon is widely used. The removal is based on physical contact between organic compound and activated carbon. After adsorption, activated carbon can be removed or regenerated. Fixed bed and moving bed reactor are usually used for this removal method. But when dealing with halogenated VOCs, this removal method is not effective. So, absorption by activated carbon is feasible for post-treatment of VOCs liquid discharges. For gaseous VOCs in air, absorption can be used but problems with activated carbon are same as the liquid VOCs operation.

Thermal oxidation is one of VOCs removal methods that is widely used in petrochemicals industries. Oxidation will occur in single ceramic chamber with use propane or natural gas as fuel. The operating temperature is 760-780 °C and maximum residence time is 1 second. However, VOCs can be used as fuel if concentration of VOCs is high. There is heat exchanger network for exchanging heat between outlet gas and inlet gas before oxidation to save the energy cost. For halogenated VOCs, gas scrubber is required for treat the exhaust gas. Thermal oxidation can remove VOCs to low level (0.1-10 g/Mm³). Catalyst can be applied in oxidation in order to reduce the operating temperature to 320-540°C. Catalyst for this reaction can be chromium oxide, nickel oxide and may even noble metals such as palladium. Thermal oxidation can be use as pre-treatment for high VOCs concentration.

UV oxidation can be operated with wastewater. Contaminants will react with strong oxidizer which are combined ozone and hydrogen peroxide. Generally, ozone is generated by low pressure 65W lamps and hydrogen peroxide is generated by

15-60W lamps. Products from UV oxidation are water, carbon dioxide and salts. This removal method can deal with wide range of VOCs concentration

2.5.2 Bio-treatment

Bio-treatment method can operate with the lowest VOCs concentration when compare with other available technologies. This technique economically and effectively treats contaminated air at 60- 150,000 m³/h flow. Advantages of bio-treatment is compact size of system so this system apply with small projects and retrofitting building easily. Existing bio-treatment of VOCs used in gas treatment revolves around the concept of bio-filtration. There are many available bio-treatment techniques such as bio-scrubbers, bio-membrane and bioreactor. Bio-filtration is based on two principals. Firstly, VOCs transfer from air to support medium. Secondly, contaminants are bio-catalysed to biomass, carbon dioxide, water and other by-products.

Traditional bio-filtration system uses fixed-bed bioreactor where the bio-catalyst or microorganism is immobilized to an inert supporting medium to develop biofilms. Ideal packing bed materials have high void fraction, light weight, low pressure drop, hydrophilic and low bulk density.

Bioscrubbers consist of an absorption tower and a bioreactor. In the absorption tower, gas phase contaminants are diffused into an aqueous solution via means of counter-current gas-liquid flows through inert packing. The washed gas is emitted from the top and the contaminated liquid pumped towards an aerated bioreactor. The microorganism or activated sludge in the reactor is suspended in a nutrient-rich media and residence time for treatment varies according to the type and concentration of VOCs in the feed. After completed degradation of contaminants, the medium is filtered and biomass left to sediment with portions being recycled through the bioscrubbing process again. An aqueous system with no high pressure drops allows for more evenly distributed temperature, nutrient and pH controls. System limitations are due to the narrow band of VOCs treatable.

For membrane bioreactors use semipermeable membrane in present of liquid and gas phase. The nutrient and biomass growth is within the liquid side whilst the gaseous contaminants are pressurized to induce diffusion over the partition into the

aqueous solution. However, membrane bioreactors for VOC treatment still require more research to minimize fouling and high cost.

2.6 Plasma

2.6.1 Plasma definition

Plasma is an electrically neutral medium of unbound positive and negative particles (i.e. the overall charge of a plasma is roughly zero). Although these particles are unbound, they are not ‘free’ in the sense of not experiencing forces. Moving charged particles generate an electric current within a magnetic field; and any movement of a charged plasma particle affects and is affected by the general field created by the motion of other charges. In turn, this governs collective behavior with many degrees of variation. Three factors are listed in the definition of a plasma stream Dendy, R. O. (1990).

2.6.2 Plasma generation

Conrads and Schmidt (2000) reviewed common methods for plasma generation. Generally, plasma is generated by applying energy to the neutral gas causing charge carrier formation. Electron and ions are produced in gas phase when energy is sufficiently supplied. There are various methods to supply energy to neutral gas to form plasma. Thermal energy is one of possibility for supply energy. Exothermic reaction of molecules is used as prime energy source. Then, adiabatic compression of gas will be used for supply energy to gas until energy level reach to point of plasma generation. Energetic beams can also use for plasma energy source. Beams of neutral particles have added advantage of being stable in electric and magnetic fields

The most commonly used method to supply energy for low-temperature plasma system is by applying electric field to a neutral gas. Electrons and ions can be found at any volume of neutral gas and those free charge carriers are accelerated by the applied electric field and new charge particles are created by colliding between free charge carriers and atoms or molecules in neutral gas. Furthermore, new charges particles can be generated by colliding between free charge carriers and surface of

electrode. These phenomena lead to avalanche of charge particles formation and they are balanced by charge carrier losses.

2.6.3 Collision processes in plasma

Electrons that have gained energy in a plasma collide with atoms and molecules. These collisions are categorized as elastic collisions and inelastic collisions. Figure 2.5 summarizes the collision processes in a plasma. With an elastic collision, only the kinetic energy changes; the internal energy does not change. This type of collision tends to take place when the electron energy is low. In the example in Figure 2.5, the electron is bounced back in a different direction. Because a portion of the electron's energy is transferred into the kinetic energy of the atom, the atom slightly gains a velocity. The electron loses a small amount of energy through the collision. With an inelastic collision, the internal energies are converted, and excitation, ionization, dissociation, and electron attachment take place. (K. Nojiri *et.al.* 2015)

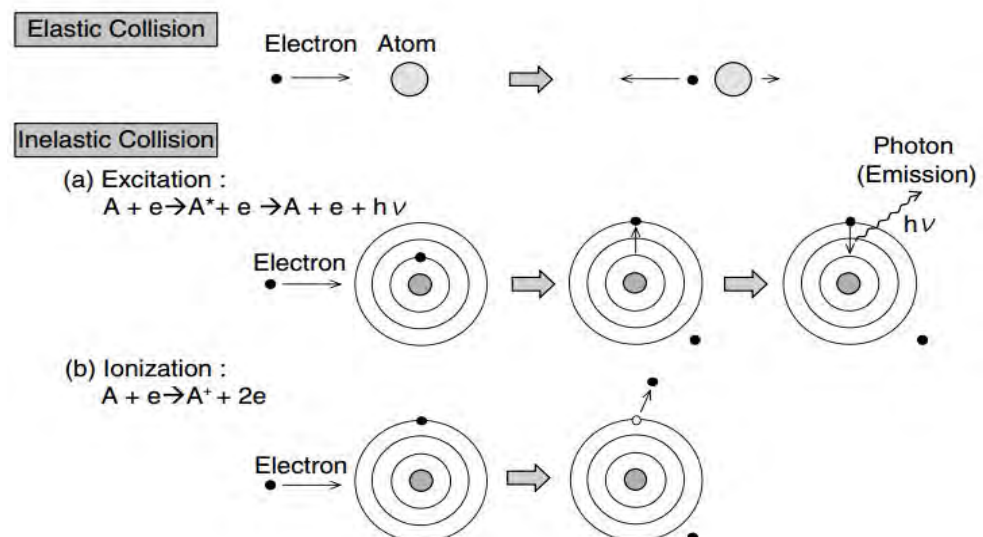
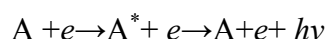


Figure 2.5 Collision processes in a plasma

2.6.3.1 Excitation

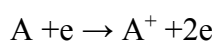
A colliding electron provides energy to the bound electron in an atom and enables it to jump to a higher energy level. In general, the excited state is unstable, and the excited electron would be able to remain in this state for only around 10^{-8} s, and then returns to the ground state. Photon is emitted during this transition. The plasma glows because of this principle. An excitation reaction step is described as follows:



where A represents a neutral atom, and A* represents A in an excited state. h is Planck's constant, and ν is the frequency of the emitted light.

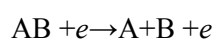
2.6.3.2 Ionization

As mentioned earlier, an electron in the outermost shell is expelled when the energy of the colliding electron is larger than the ionization voltage, and the neutral atom turns into a positive ion. This reaction step is described as follows:

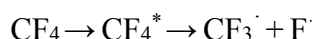


2.6.3.3 Dissociation

Dissociation occurs when the energy given by the colliding electron is larger than the binding energy of the molecule. This reaction step is described as follows:

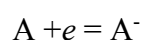


When a molecule is dissociated, its byproducts are chemically more active than the original molecule and turn into highly reactive particles. A particle in this activated state is called a radical. It has been reported that CF₄ would easily be dissociated into a CF₃ radical (CF₃·) and F radical (F·) once excited. This reaction step is described as follows:



2.6.3.4 Electron attachment

The colliding electron attaches to the atom and turns it into a negative ion. This reaction step is described as follows:



2.6.4 Plasma Classification

Plasma can be classified into two main types based on their energy level, electron density and temperature which are High temperature and Low temperature plasma (Hippler *et al.* 2017). For high temperature plasma, electrons, ions and neutral species are in a thermal equilibrium state. Low temperature plasma is further subdivided into thermal plasma (quasi-equilibrium plasma) and non-thermal plasma (non-equilibrium plasma or cold plasma).

For high temperature plasma, gas temperature (T_0) is close to electron temperature (T_e) which is very high temperature in range of 10^5 - 10^7 K. The examples of thermal plasmas are arcs and plasma torches used for the work that requires high temperature such as spraying or Inductive Coupled Plasma (ICP) for analyzing element in sample which is greater than Atomic Absorption Spectroscopy (AAS).

Temperature of low temperature plasma is lower than electron temperature ($T_0 \ll T_e$). Plasma generated by glow discharge is one of examples in this plasma type. Plasma is generated at low pressure about 1 kPa and temperature of neutral species do not change whereas electron temperature (T_e) is about 10,000 K. In this condition, plasma does not generate energy to the system but generate excited species and radicals allowing initiating and enhancing the chemical reactions. On the other hand, high temperature plasma uses electrical energy for heat gas. Hence, low temperature plasma is widely used for activating chemical reaction to occur at ambient temperature.

2.6.5 Corona discharge process

Corona discharge is widely used in ions and energetic electron producing application such as electrostatic precipitation, electrophotography static control in semiconductor industry, ionization instrumentation, control of acid gases from combustion sources, ozone generation and destruction of toxic compounds (Jen-shih *et al.*, 1991).

Corona discharges can generate the energetic species at atmospheric pressure by consuming low electrical power. Plasma can be generated by apply strong electric fields between small diameter wires, needles, or sharp edges on an electrode

and electrode plate on another side. Corona is named from “crown” by mariner’s observation of discharge on their ship’s mast during electrical storms.

The identities of produced energetic species depend on the polarity of discharge and characteristic of gas mixture. The electron energy depends on generating method and gas characteristics. In general, in application using ions, the corona induced plasma zone will occupy only small fraction of the total process volume, while a process using the electron will fill most of the volume with the plasma.

Corona discharges exist in several forms, depending on the polarity of the field and the electrode geometrical configurations. For positive corona in the needle-plate electrode configuration, discharges start with burst pulse corona and proceed to the streamer corona, glow corona, and spark discharge as the applied voltage increases. For negative corona in the same geometry, the initial form will be the Trichel pulse corona, followed by pulseless corona and spark discharge as the applied voltage increases. For a wire-pipe or wire-plate electrode configuration, corona generated at a positive wire electrode may appear as a tight sheath around the electrode or as a streamer moving away from the electrode. Corona generated at negative electrodes may take the form of a general, rapidly moving glow or it may be concentrated into small active spots called “tufts” or “beads. Figure 2.6 show the configuration of positive and negative corona discharge.

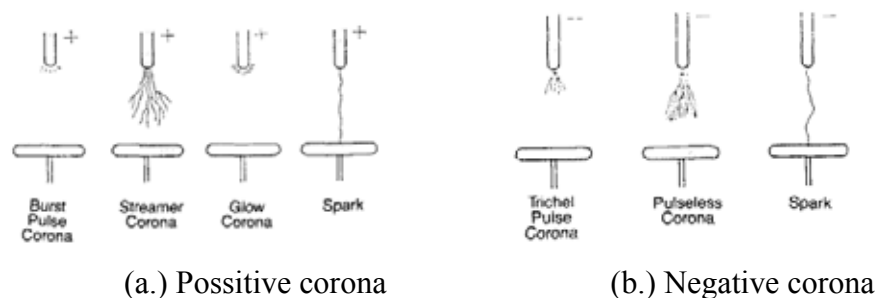


Figure 2.6 The configuration of (a.) positive and (b.) negative corona discharge

Negative corona generally propagates by impact ionization of the gas molecules. Positive corona depends more on photoionization for its propagation: the positive streamer, for example, may advance at as much as one percent of the speed of light. In either case, the ultraviolet photon flux from ion-electron recombinations is quite large.

The positive corona is characterized by a steady current at a fixed voltage, quiet operation, and almost no sparking. The positive streamer corona is a discharge confined to a narrow channel which originates at the electrode. It produces an unsteady current (because the streamer is repetitive), is quite noisy, and is the direct precursor to a spark: once streamers form at an electrode, the sparking potential has almost been reached.

The negative glow usually requires clean, smooth electrodes to form. The glow is made up of individual electron avalanches which trigger successive avalanches at nearby locations. The total current from the electrode is relatively steady, but it is composed of many tiny pulses. The discharge is noisy and the sparking potential is high compared with the positive streamer corona. The glow often changes with time into the tuft form, a process associated with the formation of more efficient mechanisms of generating successive avalanches. The tuft corona is also noisy and has a similar sparking potential to the glow form. The average current is steady, but is composed of tiny pulses like the glow corona. The tuft corona is more spatially inhomogeneous than the glow corona. Differences between negative tuft and glow coronas have been investigated recently.

2.6.6 Gliding arc discharges

As schematically shown on Figure 2.7, at least two electrodes diverging with respect to each other are placed in a relatively fast gas flow (less than 10 m/s) and in the flow direction. Gliding discharges are produced between the electrodes and across the flow. They start at the spot where the distance between the electrodes is the shortest, and spread by gliding progressively along the electrodes in the direction of flow until they disappear after a certain path. This path is defined by the geometry of the electrodes, by the conditions of flow and by the characteristics of the power supply.

The electrical discharges immediately reform at the initial spot (Czemichowski *et al.* 1994)

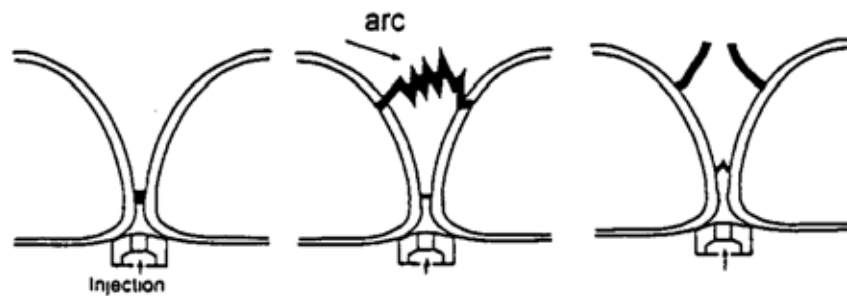


Figure 2.7 Start, life and disappearance of the gliding discharges

The displacement of the discharge roots on uncooled electrodes prevents their chemical corrosion or thermal erosion by usual high current arc establishment. The electrical energy (either DC or AC current may be used) is directly and totally transferred to the processed gas. The average voltage ranges from 0.5 to 10 kV for currents from 0.1 to 50 A (per discharge). The instantaneous voltage, current and dissipated electric per observed via digital oscilloscope show almost random feature of the history of each gliding breakdown powered by a direct current arc supply (two parallel generators: one is a high voltage generator used to ignite the discharge and the second is a power generator 800 V, 60 A). In series with the power generator there is a variable resistor 25 Ω and in order to delay the breaking off of the arc, a self-inductance 25 mH.

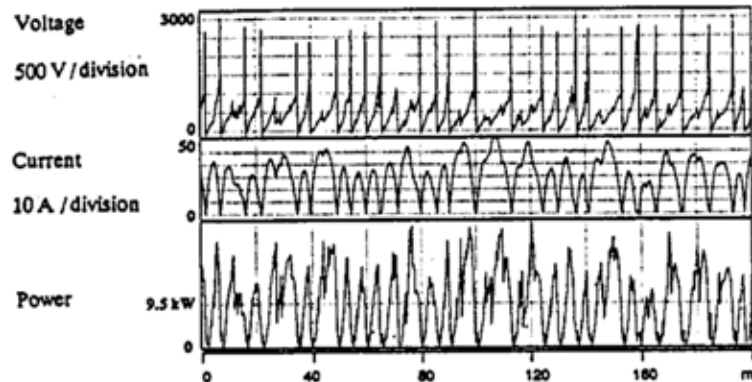


Figure 2.8 Voltage, current and power curves in 120 m³/h air flow rate (mean values: 450 V, 20 A and 9.5 kW)

The discharge starts at the shortest distance between the electrodes and within a time of dozen μ s there is formation of a low resistance plasma; the voltage falls to dozens V. The small plasma volume is then dragged by the gas flow at a speed of about 10 m/s, and both the length and voltage of the arc column increase together with the distance between the electrodes. The plasma is close to the thermodynamic equilibrium because the electrical power delivered by the generator is sufficient to compensate energy losses by thermal conduction.

Later the heat losses continue to increase, but since the electrical power cannot increase any further, it is no longer possible to sustain the arc in equilibrium. The gas temperature will fall rapidly to about 2000 - 3000 K, at the same time as the electron temperature remains at about 1 eV. These conditions are similar to those prevailing in moderate pressure high frequency discharges; the plasma conductivity is maintained by step-wise ionization processes, and the arc can continue its evolution with much smaller heat losses of 0.15 - 0.20 kW/cm. During the nonequilibrium period the dissipated power remains practically constant: 75 - 80 % of the total energy input to the arc is dissipated during this period.

The electrical energy is directly used to produce a non-equilibrium" and very reactive medium allowing efficient gas processing so that up to 45 % of this energy may be directly absorbed in an endothermic reaction. Therefore, the main innovative aspect of the gliding arc processes is certainly the way the chemical

reactions are activated via powerful electrical discharges under near-to-atmospheric pressures.

The gliding arc reactors can be implanted in many different processes that give them some advantages over conventional ones. Several applications, mostly to engineering and environment control, were already tested in laboratory and industrial scale reactors proposed for large ranges of gas flow and dissipated electric power such as air depollution of volatile organic compounds, conversion natural gas to syngas, reforming of heavy petroleum residues, CO₂ dissociation, UV generation, and decontamination of soil.

2.6.7 Dielectric barrier discharges

Dielectric-barrier discharges, or simply barrier discharges, have been known for more than a century. First experimental investigations were reported by Siemens in 1857. They concentrated on the generation of ozone. This was achieved by subjecting a flow of oxygen or air to the influence of a dielectric-barrier discharge (DBD) maintained in a narrow annular gap between two coaxial glass tubes by an alternating electric field of sufficient amplitude. The novel feature of this discharge apparatus was, that the electrodes were positioned outside the discharge chamber and were not in contact with the plasma as show in Figure 2.9 (Kogelschatz *et al.* 2002).

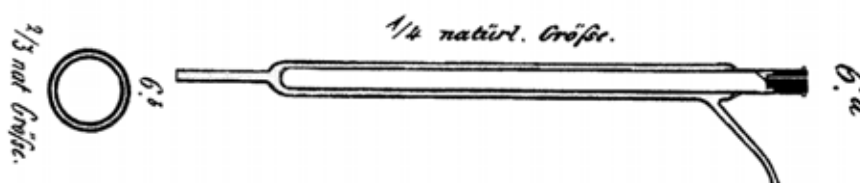


Figure 2.9 Historic ozone discharge tube of W.Siemens, 1857

Typical planar DBD configurations are sketched in Figure 2.10. As a consequence of the presence of at least one dielectric barrier these discharges require alternating voltages for their operation. The dielectric, being an insulator, cannot pass a dc current. Its dielectric constant and thickness, in combination with the time derivative of the applied voltage determine the amount of displacement current that

can be passed through the dielectrics. To transport current in the discharge gap the electric field has to be high enough to cause breakdown in the gas. In most applications, the dielectric limits the average current density in the gas space. It thus acts as a ballast which, in the ideal case, does not consume energy. Preferred materials for the dielectric barrier are glass or silica glass, in special cases also ceramic materials, and thin enamel or polymer layers. In some applications additional protective or functional coatings are applied. At very high frequencies the current limitation by the dielectric becomes less effective. For this reason, DBDs are normally operated between line frequency and about 10 MHz. When the electric field in the discharge gap is high enough to cause breakdown, in most gases many micro discharges are observed when the pressure is of the order of 10^5 Pa. This is a preferred pressure range for ozone generation, excimer formation, as well as for flue gas treatment and pollution control.

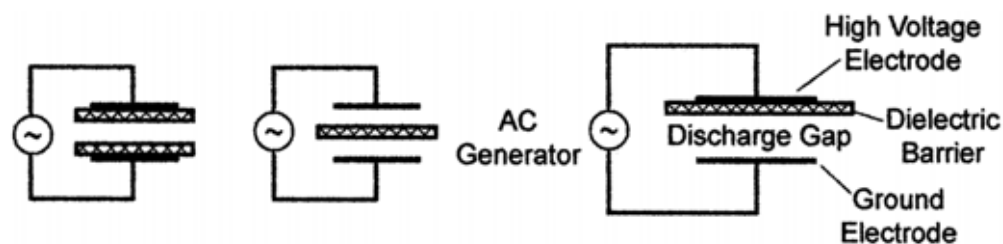


Figure 2.10 Basic dielectric-barrier discharge configurations

In this filamentary mode plasma formation resulting in electrical conductivity are restricted to the micro discharges. The gas in between is not ionized and serves as a background reservoir to absorb the energy dissipated in the micro discharges and to collect and transport the long-lived species created. In most high-power applications, liquid cooling of at least one of the electrodes is used.

DBD is a typical non-equilibrium high-pressure ac gas discharge. Recently, two types of DBD arrangements are developed; volume discharge VD and surface discharge SD. Both are beneficial for industrial because they can be operated in atmospheric and vacuum condition. Furthermore, DBD can generate the high energetic and high-density electron which 1-10 eV. Its unique advantageous is to generate low excited atomic and molecular species, free radicals and excimers with several electron volts energy. Due to its attractive characteristics, DBD is recently

widely studied for potential industrial applications. Ozone generators, excimer radiation sources, free radical generation and their applications in pollution control and monitor (Xueji Xu *et.al.*, 2001)

Michel Ondarts *et al.* (2017) have investigated the degradation of toluene and generation of by-products at low to moderate concentration (a few ppb to 1000 ppb) after flow toluene through the corona discharge which are non-thermal plasma to use corona discharge as indoor air pollution controller. They investigate effects of polarity, specific energy, inlet concentration of toluene and humidity. They have found that polarity is the greatest parameter that influence the removal efficiency.

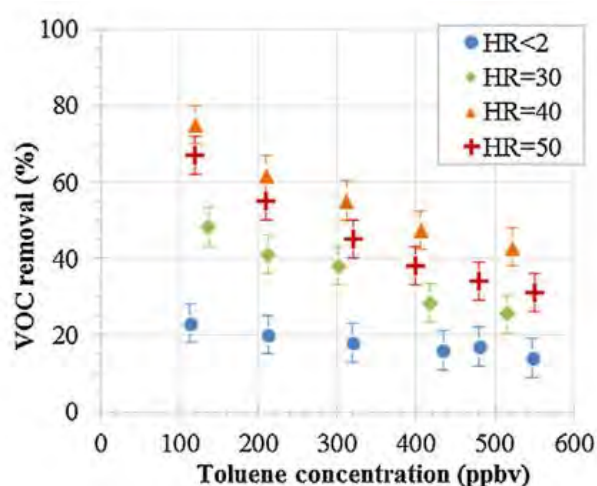


Figure 2.11 Total VOC removal as a function of inlet toluene concentration with four relative humidity levels (negative polarity, 7 kJ L^{-1} , 150 L min^{-1}).

As shown in Figure 2.11, when specific energy and humidity have been increased toluene removal efficiency will increase but when inlet concentration has been increased toluene removal efficiency will decrease. The best polarity condition for toluene is negative condition due to mobility of active species in negative polarity is higher than positive polarity.

Fada Feng *et al.* (2013) have studied the effects of applied current density and specific input energy to the toluene removal efficiency and produced ozone

concentration by using novel plasma catalysis generation base on back- corona discharge along porous catalyst bed reactor. The reactor consists of a high-voltage needle electrode, one floated mesh electrode, one catalyst bed and one grounded mesh electrode. $\text{AgMnO}_x/\text{Al}_2\text{O}_3$ -1 has been used as catalyst. The main purpose for research is to use this reactor to generate ozone and decompose volatile organic compounds.

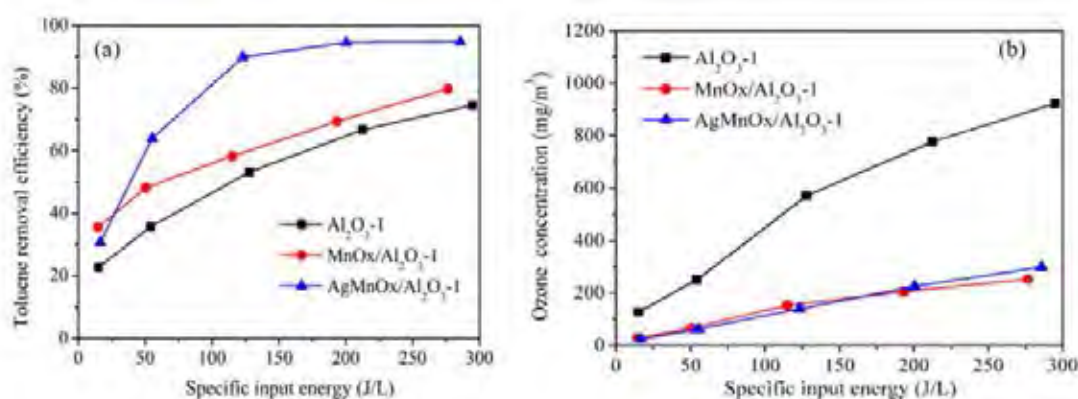


Figure 2.12 Effect of specific input energy to (a.) Toluene removal efficiency and (b.) Ozone concentration.

As shown in Figure 2.12, they have found that ozone concentration and toluene removal efficiency will increase when current density and specific input energy increase. VOCs decomposition efficiency is improved when less ozone is generated. With our home-made $\text{AgMnO}_x/\text{Al}_2\text{O}_3$ catalysts, both VOCs and its byproduct aerosols can be effectively decomposed in air. Moreover, the catalysts can be effectively regenerated on site.

Chavadej *et al.* (2007) have studied the removing volatile organic compounds (VOCs) method by using of non-thermal plasma combination with catalyst. This method is effective and economic since it can be operated at ambient condition. The main purpose of this work was to apply a combined plasma and catalytic system for VOC removal. A four-stage plasma and catalytic reactor system was set up to investigate the oxidation of gaseous benzene. Commercial TiO_2 (Degussa P25), sol-gel TiO_2 , and 1% Pt/sol-gel TiO_2 were used as catalysts in the present study.

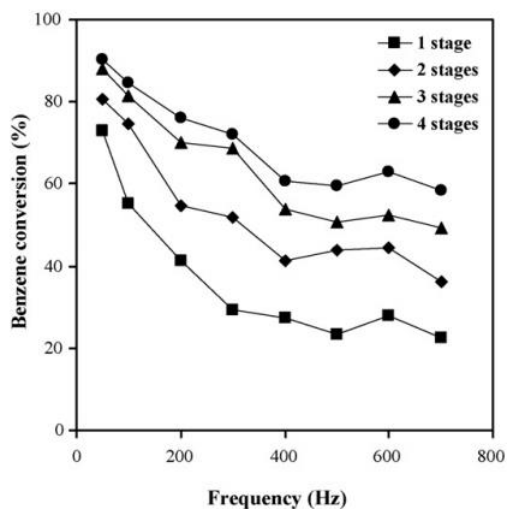


Figure 2.13 Effect of frequency on benzene conversion at different stage numbers of plasma reactors (initial benzene concentration in air = 1500 ppm; applied voltage = 21 kV; electrode gap distance = 1 cm; feed flow rate = 500 cm³/min).

Figure 2.13 illustrated the effect of frequency on benzene conversion. They found that the increasing in frequency from 50 to 700 Hz would decrease the benzene. The results could be explained that the measured current will increase with decreasing of input frequency. For any given frequency, the conversion of benzene increased with the increase in the stage number of plasma reactors. This is because the residence time is increased with the increase of the stage number. When the frequency increased, the CO selectivity increased, whereas the CO₂ selectivity conversely decreased.

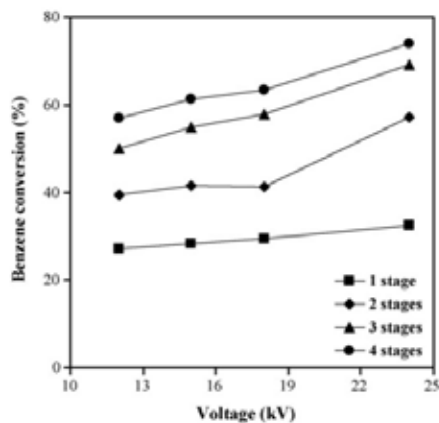


Figure 2.14 Effect of applied voltage on benzene conversion at different stage numbers of plasma reactors (initial benzene concentration in air = 1500 ppm; frequency = 300 Hz; electrode gap distance = 1 cm; feed flow rate = 500 cm³/min).

As shown in Figure 2.14, the conversion of benzene increased with increasing the applied voltage in the range of 12–24 kV, which contrasts with the effect of frequency. The explanation is that a higher voltage results in a higher electric field strength. As the applied voltage increased, the CO selectivity decreased, whereas the CO₂ selectivity increased.

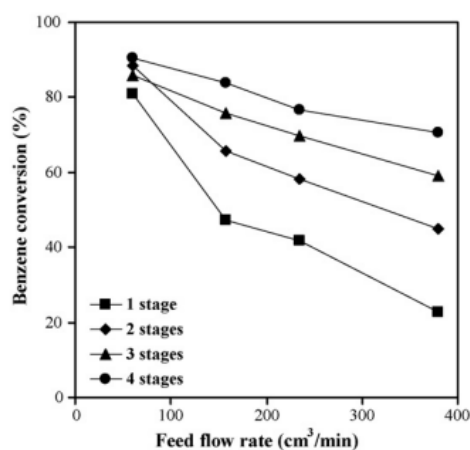


Figure 2.15 Effect of feed flow rate on benzene conversion at different stage numbers of plasma reactors (initial benzene concentration in air = 1500 ppm; frequency = 500 Hz; applied voltage = 15 kV; electrode gap distance = 1 cm).

Figure 2.15 showed the effect of the feed flow rate on benzene conversion. For any given stage number of plasma reactors in operation, the benzene conversion decreased with increasing feed flow rate because an increase in the feed flow rate directly relates to the decrease in the residence time. For any given feed flow rate, a higher stage number of plasma reactors resulted in a higher conversion of benzene. For any given stage number of plasma reactors, the CO selectivity increased with an increasing of the feed flow rate while an opposite trend was observed for the CO₂ selectivity. A higher gas flow rate or a lower stage number of plasma reactors reduces the opportunity of collision between electrons and O₂ molecules. It was apparent that all the catalysts enhanced the benzene conversion by 8% with one stage of plasma reactor and by 2% with two stages in operation.

Yajuan Wan *et al.* (2011) have studied the effects of discharge polarity, discharge electrode configuration and downstream catalyst on the removal of low-concentration formaldehyde in air were systematically investigated in a link tooth wheel-cylinder plasma reactor energized by a DC power. This research aims to control the amount of formaldehyde which is considered as primary indoor air pollution.

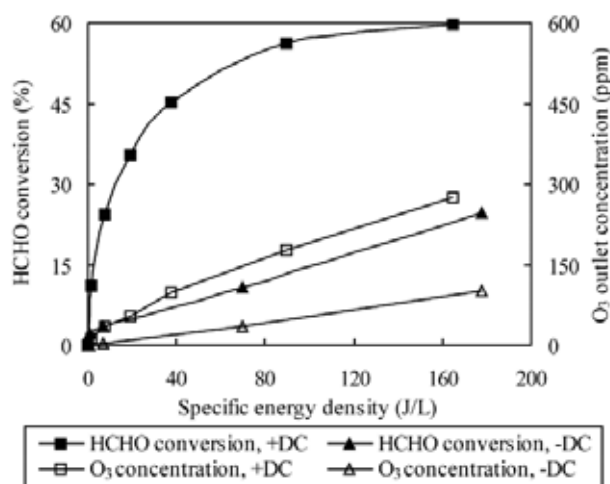


Figure 2.16 Effects of discharge polarity on formaldehyde conversion and O₃ outlet concentration.

Figure 2.16 illustrated the effect of discharge polarity on formaldehyde conversion, they found that the removal of formaldehyde by applying positive and negative DC as functions of Specific Energy Density (SED). The formaldehyde conversion increases with the increase of SED for both polarities. For a fixed SED, the

formaldehyde conversion by applying positive DC is higher than that by applying negative DC. To achieve the same formaldehyde conversion, power consumption requirement of negative DC is much larger.

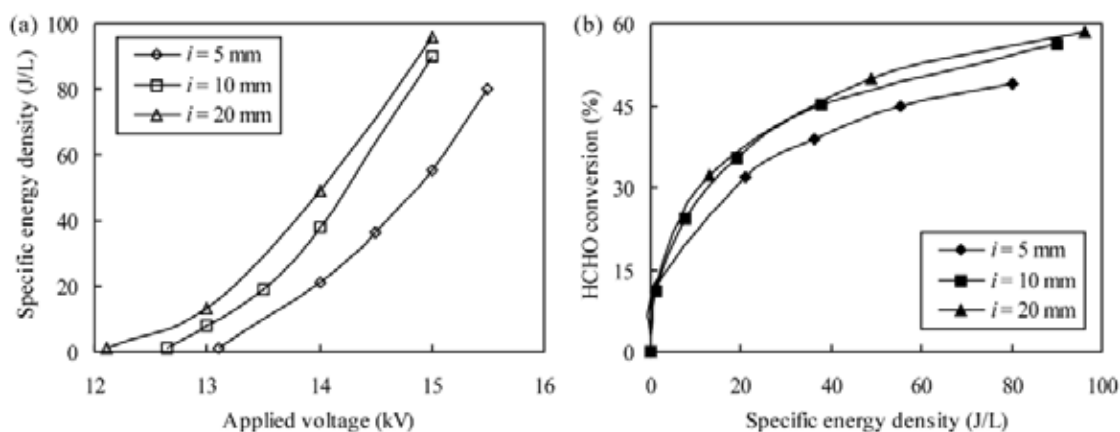


Figure 2.17 Effects of discharge tooth wheel-interval (i) on (a) energy input, and (b) formaldehyde conversion.

Results present in Figure 2.17 (a) show that under a given applied voltage, more energy can be injected into the reactor with longer interval between discharge teeth wheels. For an applied voltage of 14 kV, the SED was 21.0, 37.8 and 49.0 J/L for space intervals of 5, 10 and 20 mm, respectively. This phenomenon may be attributed to an enhanced propagation of the corona between discharge teeth wheels with longer interval. So, the formaldehyde conversion also increases with SED as show in Figure 2.17 (b).

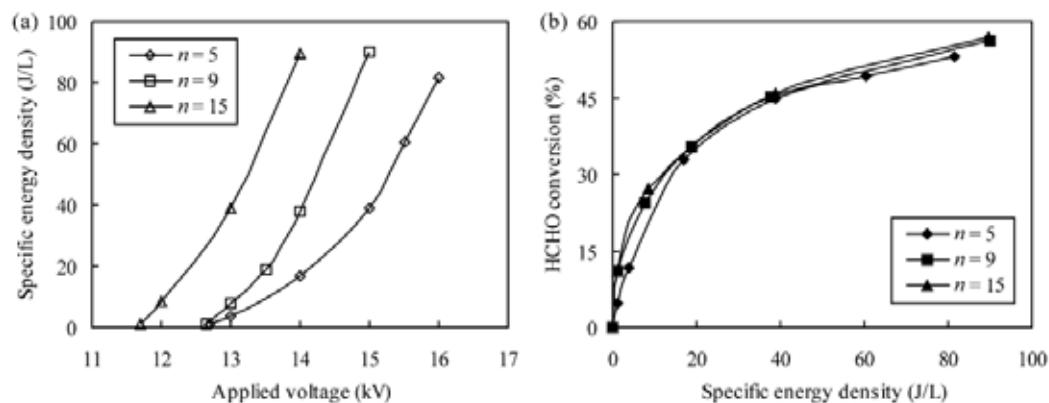


Figure 2.18 Effects of discharge tooth wheel-number (n) on (a) energy input, and (b) formaldehyde conversion.

The results from Figure 2.18, more discharge teeth wheels promote the energy input to the plasma reactor, probably due to the increasing available discharge channels. For an applied voltage of 14 kV, the SED was 16.8, 37.8 and 89.6 J/L with 5, 9 and 15 discharge teeth wheels, respectively. Despite this, more discharge teeth wheels would increase the cost of the discharge electrode. Because SED increase with tooth wheel-number so formaldehyde conversion also increases with tooth wheel-number.

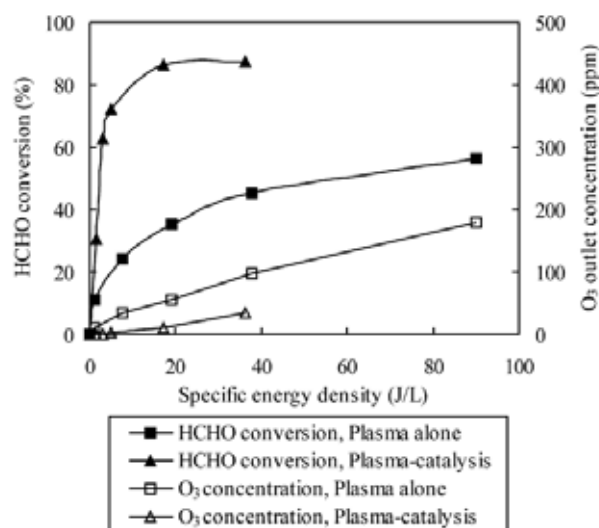


Figure 2.19 Effects of downstream catalyst on formaldehyde conversion and O₃ outlet concentration.

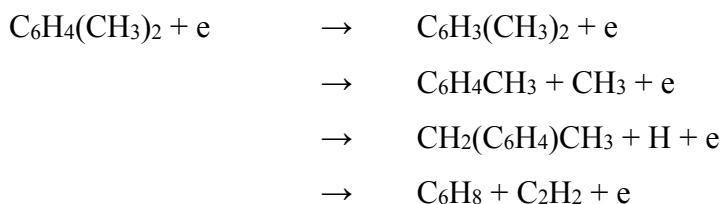
Figure 2. 19 indicates the profiles of formaldehyde conversion and O₃ outlet concentration as functions of SED for plasma process with and without downstream MnO_x/Al₂O₃ catalyst. The presence of MnO_x/Al₂O₃ catalyst significantly enhances the formaldehyde removal and reduces the O₃ emission

Jintawat Chaichanawong *et al.* (2005) have investigated the technical feasibility of using corona discharge reactions to treat high-temperature exhaust gas containing acetaldehyde and ammonia. Effect of temperature and present of water and oxygen have been studied. They found that the presence of O₂ has a significant enhancement effect on the simultaneous CH₃CHO removal efficiency. As temperature increases, the CH₃CHO removal efficiency remains nearly 100% from room temperature to 200 °C because of the effect of O₃ and O⁻ anion at low temperatures. In contrast, the CH₃CHO removal efficiency tends to significantly decrease above 200 °C because of less O₃ generated from O₂ and reduction of the mean residence time of the gas mixture inside the reactor at high temperature.

In addition, at 20% O₂, the NH₃ removal efficiency increases with temperature up to 200 °C then dramatically decreases up to 300 °C. because O₃ and O⁻ anion should contribute to the removal of NH₃ at low temperature as mention before.

Lee *et.al* (2002) had studied the p-xylene destruction path way in oxygenated and non-oxygenated system via Dielectric Barrier Discharges (DBD). The experiment was carried out at atmospheric pressure. Physical parameters investigated in this study include applied voltage, gas composition, gas flow rate, and temperature. Applied voltage was chosen as the primary control parameter which in the range of 14-16 kV due to the breakdown point and instrument limitation. Experimental runs were conducted for the simulated gas streams with p-xylene varying from 0–500 ppmv, oxygen varying from 0–20%, and water vapor varying from 0–2.3% by volume. Three gas flow rates were selected (0.5, 1.0, and 1.5 slpm) for performing the experiment. In addition, the inlet gas temperature was varied as 20 and 83 °C.

The major pathway leading to p-xylene removal in N₂ plasma is through electron impact dissociation since p-xylene does not directly react with nitrogen molecules following;



For the oxygenated system, O₂ molecules enhanced the p-xylene removal process due to reaction between O radicals and p-xylene molecules. Higher O₂ content in the gas streams led to the generation of more highly reactive O radicals in the DBD reactor, resulting in a higher removal efficiency of p-xylene. The electronegative property of oxygen tends to trigger the electron attachment reactions and changes the associated electron energy distribution. Since O₂ and N₂ are key components in the simulated gas streams, the effects of O₂ content on discharge characteristics can be evaluated by investigating their electron affinities. The electron affinities of O, O₂, N, and N₂ are 1.465, 0.43, -0.07, and -1.9 eV (electron-volt), respectively.

They conclude that electron impact was the most important channel during the discharging periods and responsible for the initial reaction for p-xylene decomposition. Radical attack was another important mechanism leading to p-xylene destruction. On the other hand, the contribution to p-xylene decomposition by ions was negligible. As the discharges were quenched, the electrons and the ions vanish, and radicals with longer lifetimes take over the destruction of p-xylene. During this gas-phase radical reaction period, the active radicals formed in discharging period govern the subsequent reactions.

The mechanism for p-xylene decomposition by radical attacks proceeds via two pathways: H atom abstraction from substituted methyl group and radical addition to the ring. The latter one, occurring roughly 90% of the time, is the more prevalent pathway. These adducts formed can further react with O₂ via H abstraction or reversible addition to form peroxy radicals, resulting in the ring opening. Possible pathways for p-xylene-OH reactions are summarized as following;

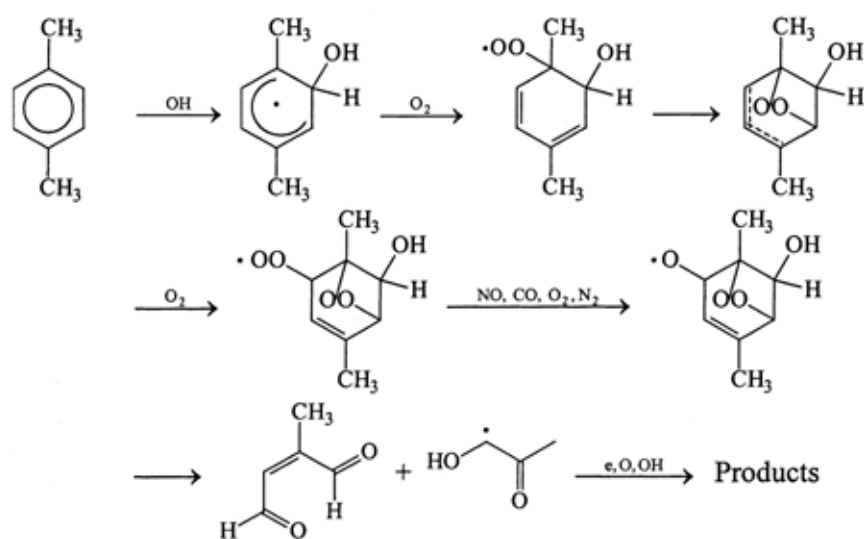


Figure 2.20 Possible path way for p-xylene-OH destruction.

Major products including CO₂, CO, CH₃CHO, and C₂H₂ are observed. The major end-product was CO₂ (approximately 70%). CO increased when DBD system was operated at a higher applied voltage. Aldehydes were the common products for the atmospheric reactions of aromatic compounds, for example, HCHO and CH₃CHO were two major products for the OH-toluene reactions.

CHAPTER III EXPERIMENTAL

3.1 Materials

Chemicals

- Benzene (AR Grade)
- Toluene (AR Grade)
- Xylene (AR Grade)
- He (UHP grade)
- Zero air (UHP grade)
- H₂ (UHP grade)
- Distillated water

3.2 Experimental Setup

The experimental system can be divided into 4 sections: reactant-carried gas section feed, plasma reactor section, power supply section, and analytical section. Figure 3.1 shows the schematic of the experimental setup for benzene, toluene and xylene (mixed VOCs) oxidation reaction using corona discharge.

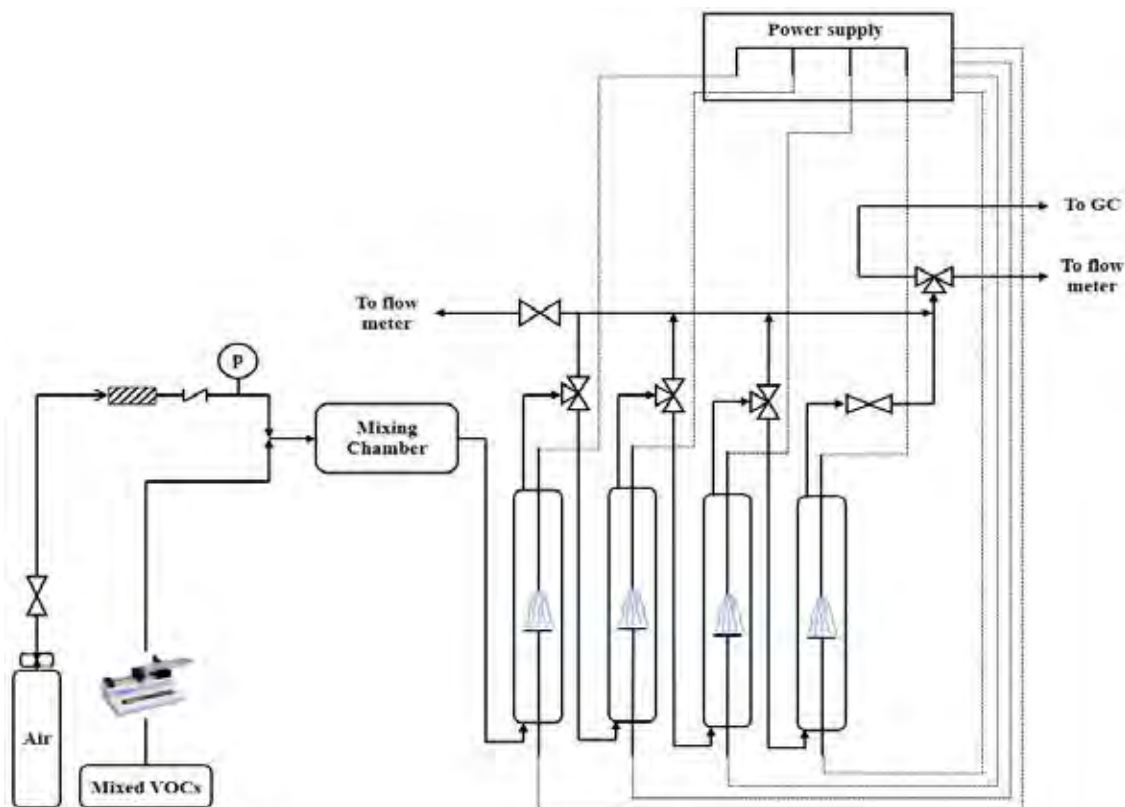


Figure 3.1 Experimental set up by using corona discharge reactors.

3.2.1 Reactant and Carried Gas Feed Section

The flow rates of the air were controlled by mass flow controllers and transducers supplied by AALBORG. The check valve was also placed downstream of each mass flow controller to prevent any backflow.

The reactant was mixture of benzene, toluene and xylene at 1:1:1 by mole respectively. The reactant concentration was achieved by vaporizing benzene, toluene and xylene (mixed VOCs) at a controlled temperature of 120 °C. The flow rate of mixed VOCs was controlled by a syringe pump supplied. To prevent the any product condensation, the temperature of stainless tube in plasma reactors section to the GC detector was maintained at 120 °C by using a heating cable.

3.2.2 Reactor Section

For the plasma oxidation of mixed VOCs, the non-thermal plasma reactor used in this experiment is corona discharges which are connected in series. These reactor schematics are shown in Figure 3.2.

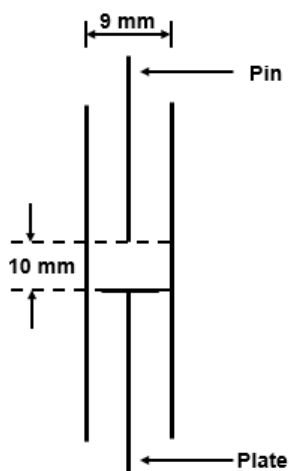


Figure 3.2 Configuration of corona discharge reactor.

The corona discharge reactor comprised of a 20-centimeter-long quartz tube with an outer diameter of 9 mm and an inner diameter of 7 mm. Plasma was generated between pin and plate electrodes, which were located at the center of the reactor tube and the electrode gap distance is 10 mm.

3.2.3 Power Supply Section

The power supply unit consisted of three steps. For the first step, a domestic AC input of 220 V and 50 Hz was converted to a DC output of 70 V by a DC power supply converter. For the second step, a 500 W power amplifier with a function generator was used to convert the DC into AC current with a sinusoidal waveform and different frequencies. For the third step, the outlet voltage was stepped up by using a high voltage transformer. The output voltage and frequency were controlled by the function generator. The voltage and current at the low voltage side were measured

instead of those at the high voltage side by using a power analyzer since the plasma generated is non-equilibrium in nature. The high side voltage and current were thereby calculated by multiplying and dividing by a factor of $15,000/220 \sim 68.2$, respectively. Figure 3.3 shows the electric diagram of the power supply unit used in this study.

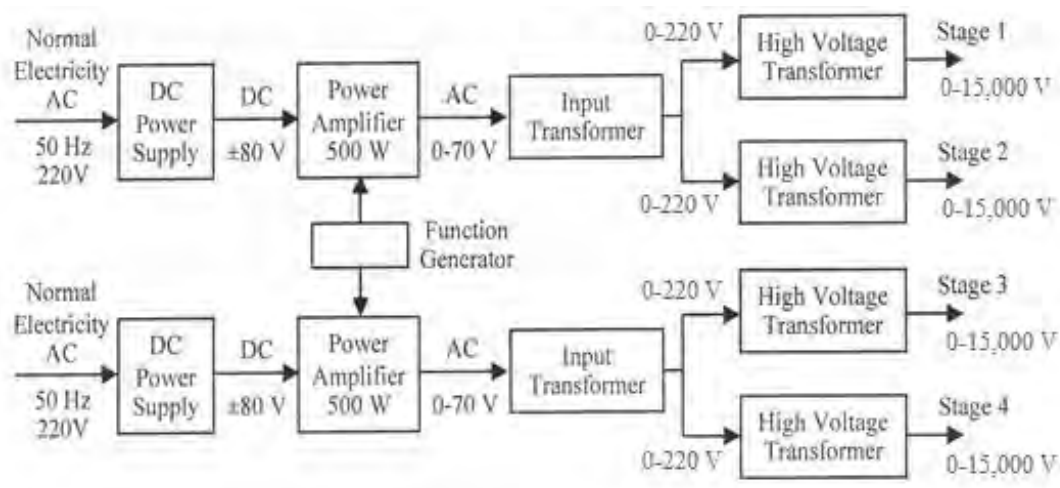


Figure 3.3 Schematic of the power supply unit.

3.2.4 Analytical Section

Composition of gas before and after the reaction in all experiments, the effluent gas samples were analyzed by an on-line gas chromatograph (HP, 5890) equipped with a thermal conductivity detector (TCD) and a flame ionization detector (FID). The quantitative analysis of the percent volumes of all gaseous components was carried out by correlating their peak area responses obtained from the GC chromatograms. The gas chromatograph was equipped with a 10-port valve in order to separate the gas sample into two parts with independent sample loops. The first part was flow through a Carboxen 1000 column with the TCD. The second part was fed into a Rtx®-5 column connected with the FID. The GC conditions are summarized as follows:

Injector type:	Automatic sampling valve (programmable)
Injection temperature:	190°C
Oven temperature:	Initial temperature 40°C, ramp up at 10°C/min to 180°C followed and then hold for 5 min
Detectors:	Thermal conductivity detector (TCD) and flame ionization detector (FID)
Detector temperature:	250°C
GC columns:	Carboxen 1000 (15' x 1/8') and Rtx®-5 (30 m x 0.53 mm)
Carrier gas:	High purity helium (99.995%)
Carrier gas flow rates:	35 cm ³ /min for Carboxen 1000 column and 105 cm ³ /min for Rtx®-5 column

3.3 Experimental Procedure

3.3.1 The Experimental System

- 1) Set up plasma reactor and all equipment to system as shown in Figure 3.1 Adjust the temperature controls for heating line before input and output temperature of plasma reactor to 150 °C and 200 °C, respectively. Then, open zero grade air into plasma reactor.
- 2) Prepare sample reactants of mixed VOCs which is tested in the form of liquid using syringe then inject to system by syringe pump. Adjust injection flow rate to constantly concentration of mixed VOCs at 300 ppm in zero air gas.
- 3) Adjust flow rate of zero air by digital mass flow controller.
- 4) Measure feed flow rate before reaction outing from reactor by mass flow meter and analyze composition of mixing gas by Gas chromatography.
- 5) Turn on power supply unit and set applied voltage equal to 220 kV and frequency 50 Hz from function generator to plasma system, then observe the characteristics of plasma between electrodes.
- 6) Wait until plasma reach steady state about 10 minutes.

- 7) Detect gas after oxidation reaction to analyze composition of gas by Gas chromatography every 30 minute until the result stable (SD less than 5%)
- 8) Turn off power supply unit, close valves of zero air, turn off switch mass flow controller and gradually reduce temperature of temperature control.
- 9) Clean gas remaining in line pipe and reactor about 15 minutes.
- 10) Take off reactor, clean electrodes and surface inside the reactor.

3.4 Reaction Performance Evaluation

The plasma system performance was evaluated from mixed VOCs conversions, CO₂ and CO selectivity and specific energy consumption. The conversion of reactant defined as:

$$\text{Reactant conversion (\%)} = \frac{\text{mole of reactant in} - \text{mole reactant out}}{\text{mole of reactant in}} \times 100$$

$$\text{Benzene conversion (\%)} = \frac{\text{mole of benzene in} - \text{mole benzene out}}{\text{mole of benzene in}} \times 100$$

$$\text{Toluene conversion (\%)} = \frac{\text{mole of toluene in} - \text{mole toluene out}}{\text{mole of toluene in}} \times 100$$

$$\text{Xylene conversion (\%)} = \frac{\text{mole of xylene in} - \text{mole xylene out}}{\text{mole of xylene in}} \times 100$$

The selectivity of CO and CO₂ is calculated as follow:

$$\text{Selectivity of CO (\%)} = \frac{\text{mole of CO in a product}}{(6 \times \text{mole of } C_6H_6 \text{ converted}) + (7 \times \text{mole of } C_7H_8 \text{ converted}) + (8 \times \text{mole of } C_8H_8 \text{ converted})} \times 100$$

$$\text{Selectivity of CO}_2 \text{ (\%)} = \frac{\text{mole of CO}_2 \text{ in a product}}{(6 \times \text{mole of } C_6H_6 \text{ converted}) + (7 \times \text{mole of } C_7H_8 \text{ converted}) + (8 \times \text{mole of } C_8H_8 \text{ converted})} \times 100$$

$$\text{Carbon balance of output products (\%)} = \frac{C_{pi}[P_i]}{C_{Ri}[R_i]} \times 100$$

Where	[P]	=	Mole of product in the outlet gas stream
	[R]	=	Mole of each reactant in the feed stream
	C _P	=	Number of carbon atoms in a product molecule
	C _R	=	Number of carbon atoms in a reactant molecule

The specific energy consumption is calculated in a unit of W.s per molecule of converted toluene using the following equation:

$$\text{Specific energy consumption} = \frac{P \times 60}{N \times M_c}$$

where P = power measured at the low voltage side of the power supply unit
(W)

N = Avogadro's number (6.02×10^{23} molecule g mole⁻¹)

M = rate of converted carbon in the rate of produced CO₂ molecules
(g mole min⁻¹)

CHAPTER IV

RESULTS AND DISCUSSION

4.1 Condensed Products Analysis

Figure 4.1 shows the chromatograms of GC-MS analysis of condensed products from oxidation reaction of mixed VOCs by corona discharge. In order to obtain a better understanding of decomposition of mixed VOCs, the possible degradation pathways of p-xylene have been performed as mentioned in the introduction. There is report that there are two main collision steps consisting of electron collision and oxygen radical attraction. The condensed products were corrected at an applied voltage of 4 kV, an input frequency of 600 Hz. As show in figure 4.2, the condensed products were both of cyclic and noncyclic oxygenated molecules. The detected condensed products from GC-MS were in following order: formic acid, acetic acid, acetic anhydride, 2-cyclopente-1-one, phenol, p-benzoquinone, benzaldehyde, benzyl alcohol, 1,4-cyclohex-2-ene dione and 3-methylbenzyl alcohol. The main composition of condensed products was acetic acid. From the results, it could be confirmed that two earlier mention steps occurred because all condensed products contain at least one oxygen atom in molecule.

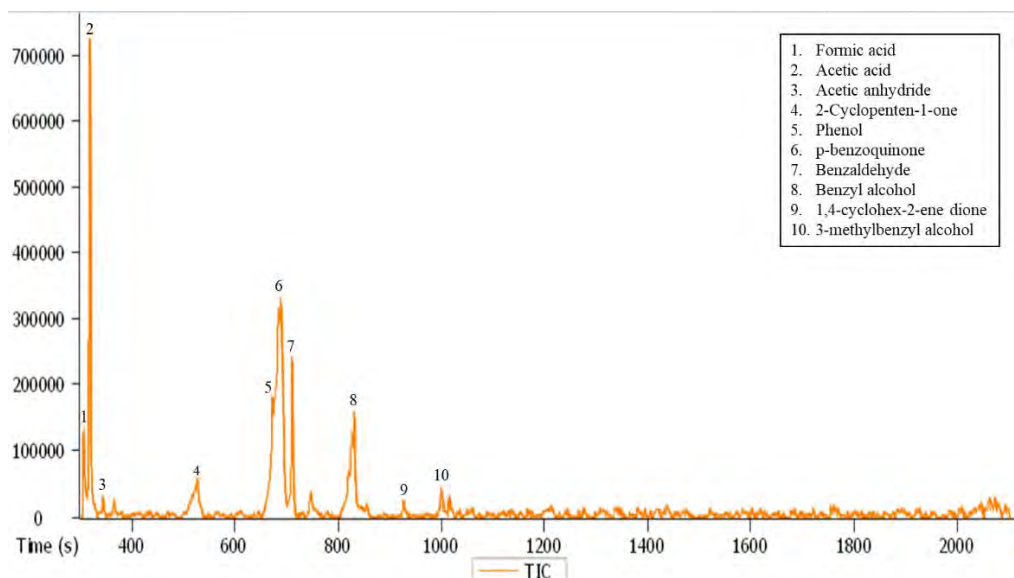


Figure 4.1 Chromatogram of GC–MS analysis for mixed VOCs degradation products by corona discharge at an applied voltage of 4 kV, an input frequency of 600 Hz, an initial concentration of 100 ppm and reactant feed flow rate of 50.0 ml/min.

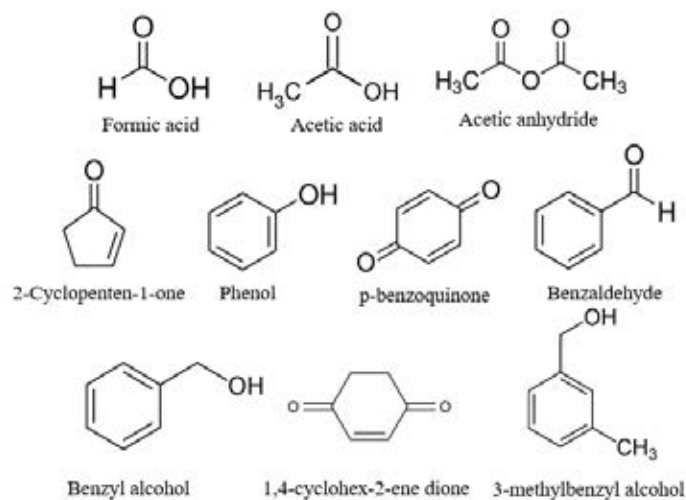


Figure 4.2 Summary of products of the studied mixed VOCs oxidation by corona discharge at an applied voltage of 8 kV, an input frequency of 400 Hz, an initial concentration of 100 ppm and reactant feed flow rate of 50.0 ml/min.

4.2 Effect of Applied Voltage

An applied voltage is one of important parameters that play a significant role on plasma chemical performance and behaviors (Feng *et al.*, 2013). Due to the instrument limitation, the generated voltage could be varied in range of 3 to 15 kV. The operationalable applied voltage was in the range of 4 to 10 kV. Despite of coke formation leading to non-stable plasma formation, the highest operationable voltage was 10 kV. Due to plasma could not be generated, the lowest operationable an applied voltage was 4 kV. The input frequency was varied at 300, 400, 500 and 600 Hz. The VOCs initial concentration and reactant feed flow rate were fixed at 100 ppm and 50.0 ml/min respectively.

4.2.1 The Effect of Applied Voltage on Reactant Conversion

The effect of applied voltage on VOCs conversion was illustrated in Figure 4.3. At any studied input frequency, the VOCs conversion increased with increasing an applied voltage. As show in Figure 4.4, the measured current across electrodes increased while the applied voltage was increasing. These phenomena led to the more generated electrons and produced active species resulting to the higher VOCs conversion. The highest VOCs conversion of 97.38% was observed at an applied voltage of 10 kV.

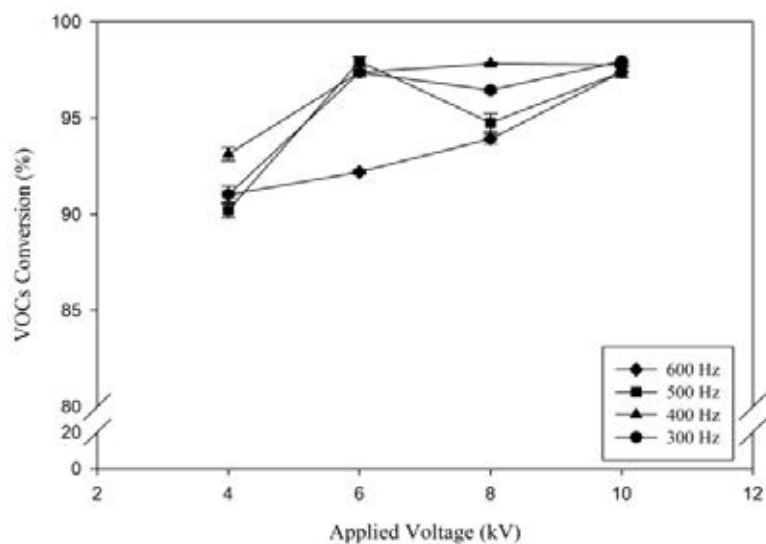


Figure 4.3 Effect of applied voltage on VOCs conversion at initial VOCs concentration 100 ppm, reactant feed flow rate of 50.0 ml/min and input frequency of 300 (●), 400 (▲), 500 (■) and 600 Hz (◆).

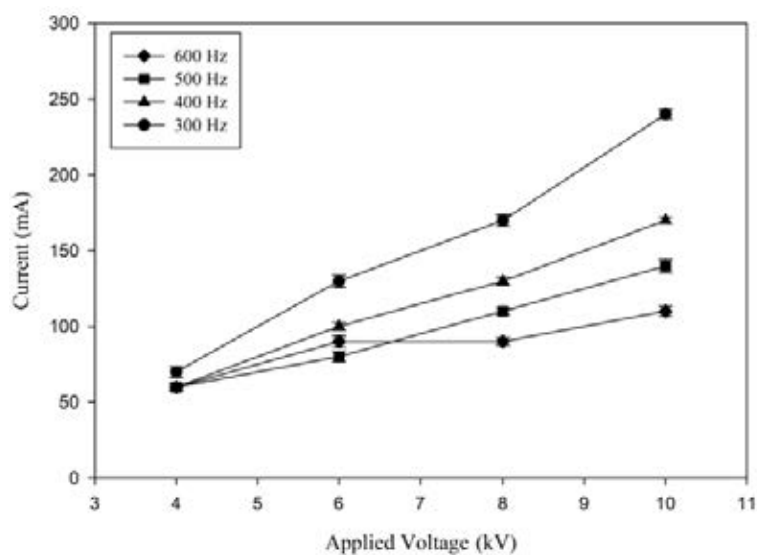


Figure 4.4 Effect of applied voltage on measured current across electrodes at an input frequency of 300 (●), 400 (▲), 500 (■) and 600 (◆).

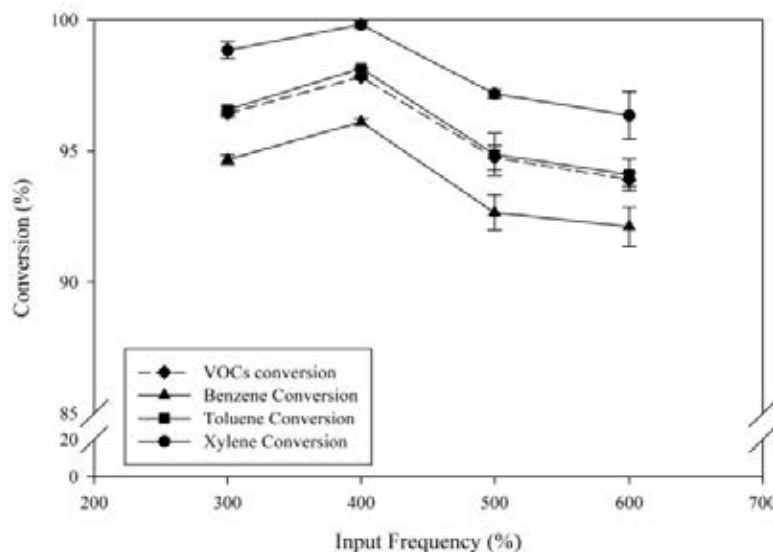


Figure 4.5 Effect of input frequency on VOCs (dash line), benzene (\blacktriangle), toluene (\blacksquare) and xylene (\bullet) conversion at initial VOCs concentration 100 ppm, reactant feed flow rate of 50.0 ml/min, an applied voltage of 8 kV and input frequency of 300, 400, 500 and 600 Hz.

Figure 4.5 illustrate effect of input frequency on VOCs dash line, benzene, toluene and xylene conversion at an applied voltage of 8 kV. Results showed that at any studied input frequency, the conversion were in following order: xylene, toluene and benzene. According to the proposed mechanism, there are three path ways of reaction in plasma zone consisting of electron collision, ion attraction and oxygen radical attraction. By the way, there were only main existing steps which were electron collision and oxygen radical attraction. In electron collision step, there was an opportunity of collision between xylene molecules and generated electron which produce both of $C_6H_4CH_3$ and C_6H_8 . For toluene molecules, they probably collided with generated electrons and had an opportunity to produce C_6H_8 (Lee *et al.* 2002). At studied condition, benzene, toluene, xylene and VOCs conversion at an input frequency of 500 Hz were found to be 96.11, 98.15, 99.82 and 97.83% respectively.

4.2.2 The Effect of Applied Voltage on CO and CO₂ selectivity

Figure 4.6 shows the effect of applied voltage on CO and CO₂ selectivity. The results show that the CO selectivity decreased while the applied voltage was increasing. On the contrary, CO₂ selectivity increase with increasing the applied voltage. The results can be explained by fundamental concept of plasma generation that there are more produced electrons in plasma environment from electrodes when the applied was increased. This phenomenon can be confirmed by the increasing in measured current across electrodes when an applied voltage was increased as shown in Figure 4.5. The increase in current while an applied voltage was increase resulting the increasing of generated electrons provided the higher opportunity for VOCs molecules to react with generated electrons themselves and produced active species such as O⁻ leading to a higher VOCs conversion and CO₂ selectivity (Chavadej *et al.*, 2007). According to the increasing of current in system, CO which can be considered as by product of this oxidation reaction also further reacted with produced active species and further produced CO₂ resulting to the increasing of CO₂ selectivity. Therefore, at an applied voltage of 8 kV and input frequency of 400 Hz showed the good VOCs oxidation performance which provide the high CO₂ selectivity which was 88.04% and low CO selectivity which was 7.56% as same as the effect of input frequency.

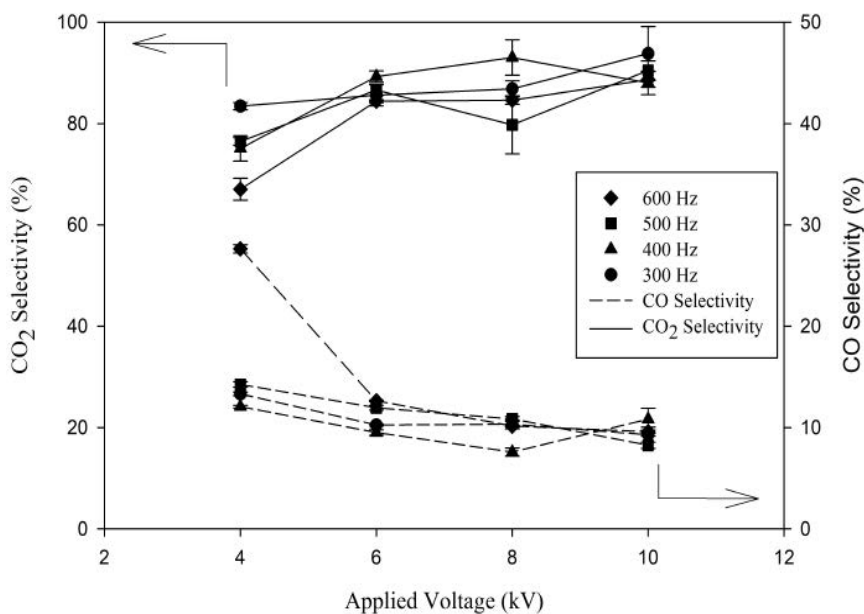


Figure 4.6 Effect of applied voltage on CO₂ (solid line) and CO (dash line) selectivity at initial concentration at 100 ppm, reactant feed flow rate of 50.0 ml/min and input frequency of 300 (●), 400(▲), 500 (■) and 600(◆).

4.3.3 The Effect of Applied Voltage on Power Consumption

The effect of applied voltage on power consumption to convert one molecule of VOCs is shown in Figure 4.7. It showed that the power consumption decreased while an applied voltage in the operationable range of 4 to 10 kV was increasing. In addition, at an applied voltage of 8 kV could be considered as an optimum applied voltage due to the lower power consumption when compared to another applied voltage at fixed input frequency.

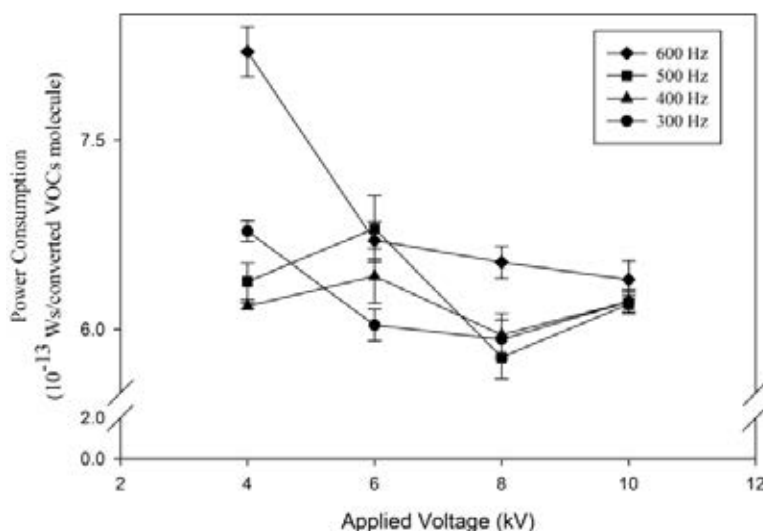


Figure 4.7 Effect of applied voltage on power consumption at initial VOCs concentration at 100 ppm, reactant feed flow rate of 50.0 ml/min and input frequency of 300 (●), 400 (▲), 500 (■) and 600 (◆).

4.3 The Effect of Input Frequency

Basically, the input frequency has significantly impacts to the electric field strength in the plasma zone. The VOCs oxidation performance was investigated by varying input frequency from 300 to 600 Hz whereas other operating parameters were fixed at an initial VOCs concentration in air of 100 ppm and total feed flow rate of 50.0 ml/min. The applied voltage was varied as 4, 6, 8, and 10 kV respectively. The limitation of the operationable lowest frequency of 300 Hz was due to the coke formation leading to the non-stable plasma formation. Whereas, the input frequency higher than 600 Hz, plasma cannot occur.

4.3.1 The Effect of Input Frequency on Reactant Conversion

Figure 4.8 illustrates the effect of input frequency on VOCs conversion. At any applied voltage, the VOCs conversion decreased with increasing input frequency. According to the basic concept of the frequency which affect to the characteristics of alternating current discharge by changing the plasma reaction performance and behaviors (Chavadej *et al.*, 2006). For alternating current system, frequency represent the cycle loop over time to change polarity from positive to negative and from negative to positive between electrodes within short time. The lower frequency, the lower reversal rate of electric field leading to the higher current in plasma system which resulted to the increasing of collision opportunity between electrons and O₂ molecules. Therefore, there are more active species in the system which further react with VOCs molecules (Chang *et al.*, 1991). At an input frequency of 300 Hz showed the highest VOCs conversion which was 97.38% at an applied voltage of 10 kV. These results were well correlated with the decreasing in current with increasing input frequency at any studied applied voltage as shown in Figure 4.9.

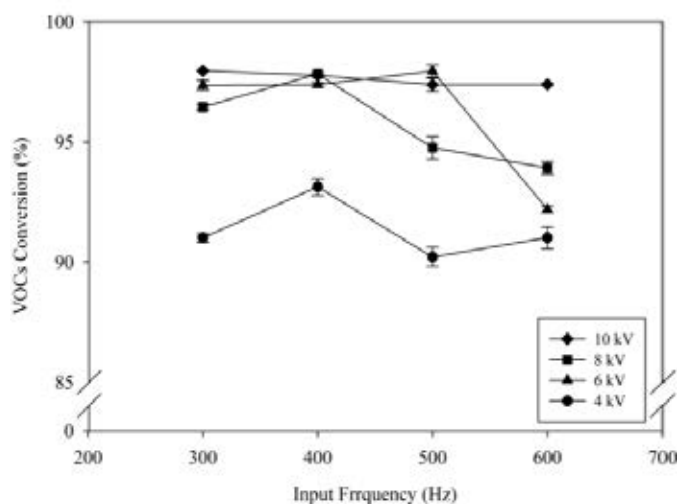


Figure 4.8 Effect of input frequency on VOCs conversion at initial VOCs concentration 100 ppm, reactant feed flow rate of 50.0 ml/min and applied voltage of 4 kV (●), 6 kV (▲), 8 kV (■) and 10 kV (◆).

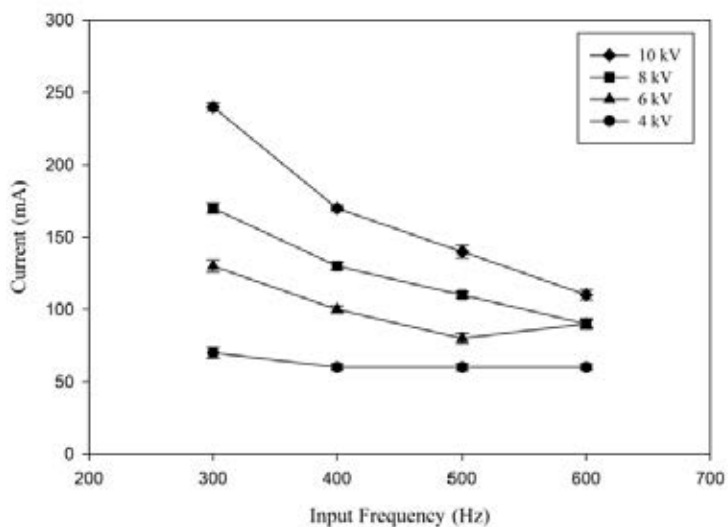


Figure 4.9 Effect of input frequency on measured current across electrodes at an applied voltage of 4 kV (●), 6 kV (▲), 8 kV (■) and 10 kV (◆).

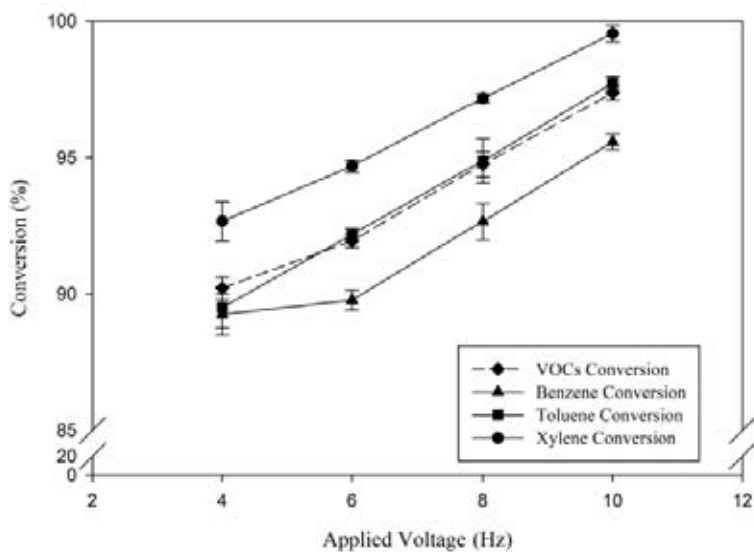


Figure 4.10 Effect of applied voltage on VOCs (dash line), benzene (▲), toluene (■), and xylene (●) conversion at initial VOCs concentration 100 ppm, reactant feed flow rate of 50.0 ml/min, an input frequency of 500 Hz and applied voltage of 4, 6, 8 and 10 kV.

Figure 4.10 showed effect of applied voltage on VOCs, benzene, toluene, and xylene conversion at an input frequency of 500 Hz. Aforementioned, toluene has a collision opportunity with generated electron to produce both $C_6H_4CH_3$ and C_6H_8 molecules as products and $C_6H_4CH_3$ molecules has a collision opportunity to produce only C_6H_8 molecules. Therefore, the xylene conversion would higher than toluene and xylene conversion respectively as well as at an optimum applied voltage of 8 kV. At an applied voltage of 10 kV, benzene, toluene, xylene and VOCs conversion at an applied voltage of 8 kV found to be 95.58, 97.73, 99.55 and 97.38% respectively.

4.3.2 The Effect of Input Frequency on CO and CO₂ Selectivity

Figure 4.11 show the effect of input frequency on CO and CO₂ selectivity. The increasing of input frequency resulting in decreasing of CO₂ selectivity but CO selectivity increased. As confirmed in Figure 4.9, the higher input frequency was the lower current lead to the less generated electrons and produced active species. Therefore, the reaction between produced active species and CO molecules did not occur frequently when compared to the system with higher current. Thus, at an input frequency of 400 Hz and applied voltage of 8 kV performed the appropriate performance considering from trace amount of CO selectivity. At this condition, only 7.56% of CO selectivity was produced at high CO₂ selectivity of 88.04%.

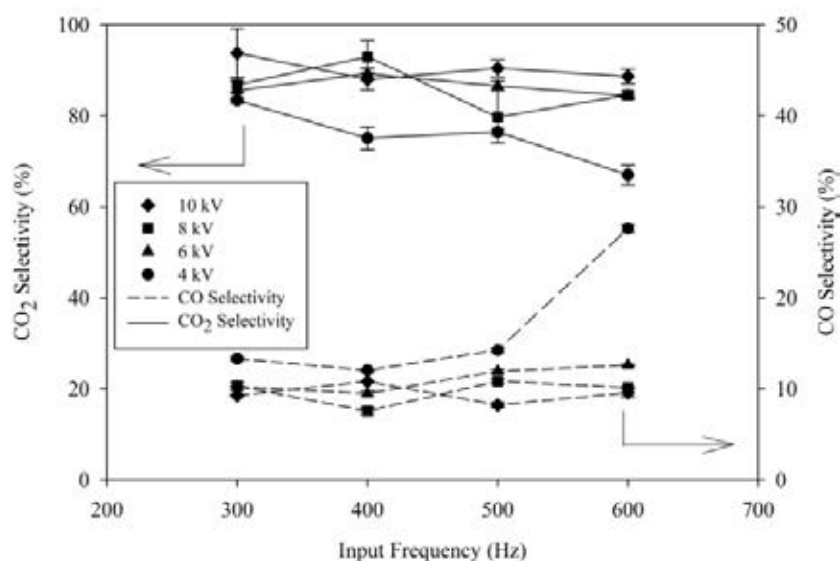


Figure 4.11 Effect of input frequency on CO₂ (solid line) and CO (dash line) selectivity at initial concentration at 100 ppm, feed flow rate of 50.0 ml/min and applied voltage of 4 kV (●), 6 kV (▲), 8 kV (■) and 10 kV (◆).

4.3.3 The Effect of Input Frequency on Power Consumption

The effect of input frequency on power consumption to convert one molecule of VOCs was illustrated in Figure 4.12. From the overall results, the operationable condition at an applied voltage of 8 kV and input frequency of 400 Hz seemed to be an appropriate operationable condition in point of high VOCs conversion, CO₂ selectivity and low CO selectivity. However, when the effect of input frequency on power consumption was considered, an applied voltage of 8 kV and input frequency of 400 Hz did not provide the suitable operationable condition. This condition consumed a quite high energy when compared to another studied operationable condition. When the effect of CO and CO₂ selectivity and power consumption were combined together, it could be concluded that at an applied voltage of 8 kV and input frequency of 500 Hz was an optimum operationable condition that not only consumed less energy but also provided the high VOCs conversion, CO₂ selectivity and low CO selectivity. At this operationable condition, VOCs conversion was 94.76% and CO₂ and CO selectivity were found to be

89.75% and 10.84% respectively. Therefore, an applied voltage at 8 kV and input frequency of 500 Hz would be selected as an optimum operationable condition for further investigating the effect of the reactant feed flow rate and the stage number.

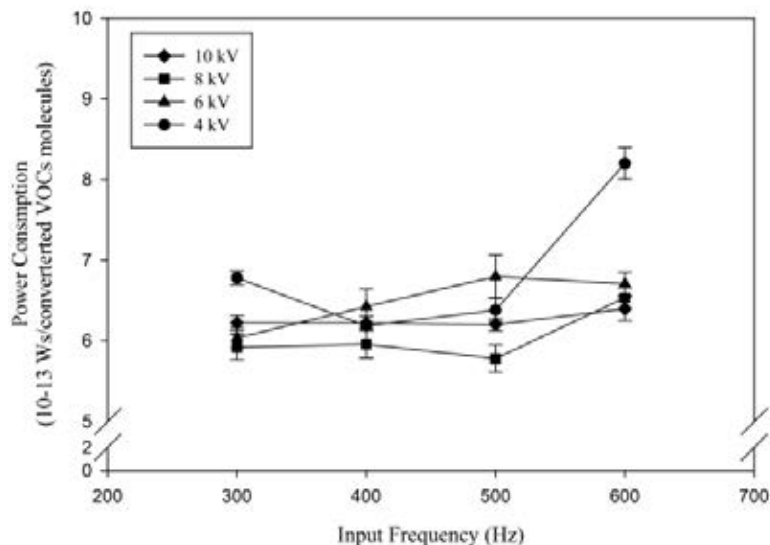


Figure 4.12 Effect of input frequency on power consumption at initial VOCs concentration at 100 ppm, reactant feed flow rate of 50.0 ml/min and applied voltage of 4 kV (●), 6 kV (▲), 8 kV (■) and 10 kV (◆).

4.4 The effect of Feed Flow Rate

Fundamentally, the changing of reactant feed flow rate directly affects the residence time of reactant in plasma zone. The effect of reactant feed flow rate (or residence time) on VOCs conversion, CO and CO₂ selectivity at an optimum operationable condition which was 8 kV and 500 Hz were illustrated in Figure 4.9 and 4.10 respectively. In this study, reactant feed flow rate was varied as 25, 50, 75, 100 and 125 ml/min corresponding to the residence time of 0.92, 0.46, 0.31, 0.23 and 0.19 second respectively.

4.4.1 The Effect of Reactant Feed Flow Rate on Reactant Conversion

Figure 4.13 showed that the increasing of reactant feed flow rate resulted to the decreasing of VOCs conversion which dramatically dropped from 97.7% to 63.9% when the reactant feed flow rate was increased from 50 to 125 ml/min. Aforementioned, the changing of reactant feed flow rate would directly affect to the residence time. The decreasing of residence time referred to the decreasing in period of the VOCs molecules stay in the plasma zone leading to lowering in opportunity for VOCs molecules to collide with produced active species (Ye *et al.*, 2008). Furthermore, the results also showed that the xylene conversion would higher than toluene and xylene conversion respectively.

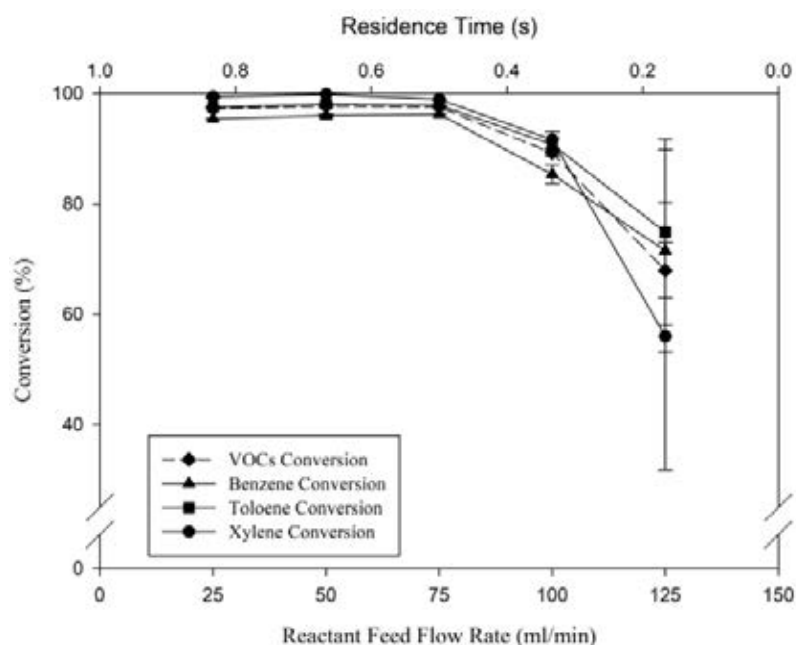


Figure 4.13 Effect of reactant feed flow rate on VOCs (dash line), benzene (\blacktriangle), toluene (\blacksquare), and xylene (\bullet) conversion at applied voltage of 8 kV, input frequency of 500 Hz and initial VOCs concentration 100 ppm.

4.4.2 The Effect of Reactant Feed Flow Rate on CO and CO₂ Selectivity

The changing of feed flow rate also affected to CO and CO₂ selectivity. As shown in Figure 4.14, the CO₂ selectivity increased when reactant feed flow rate was decreased while CO selectivity continuously decreased. The results can be explained by the increasing of residence time when reactant feed flow rate was increased. It showed that CO₂ selectivity was increased from the reactant feed flow rate of 25 to 50 ml/min. However, it dramatically dropped from 84% to 22% when the reactant feed flow rate was increased from 50 to 125 ml/min. Additionally, the CO selectivity slightly decreased with increasing reactant feed flow rate from 25 to 50 ml/min. While further increasing of reactant feed flow rate from 25.0 to 50.0 ml/min, the CO selectivity increased from 8% to 62%. The results can be explained by the fact that the higher residence time provided the more period CO of molecules stay in plasma zone which can be considered as by product for this oxidation reaction in plasma zone resulting to the more collision opportunity between CO and produced active species becoming to CO₂ molecules. Therefore, the CO selectivity decreased with decreasing reactant feed flow rate.

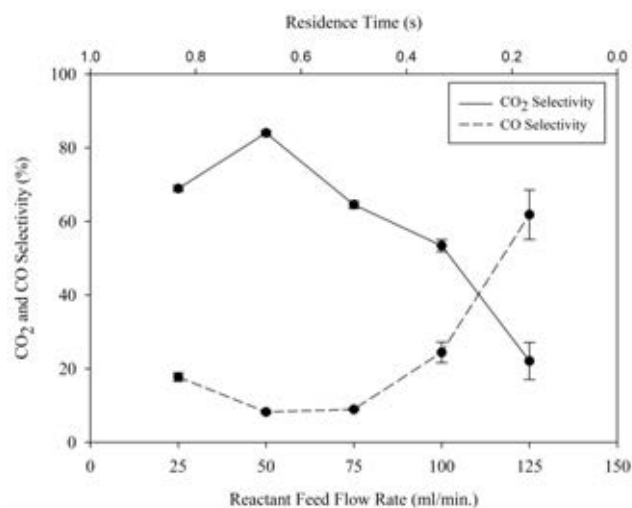


Figure 4.14 Effect of reactant feed flow rate on CO₂ (solid line) and CO (dash line) selectivity at applied voltage of 8 kV, input frequency of 500 Hz and initial concentration at 100 ppm.

4.4.3 The Effect of Reactant Feed Flow Rate on Power Consumption

Figure 4.15. illustrated the effect of reactant feed flow rate on power consumption. The results show that the energy consumption continuously decreased with the increasing of the reactant feed flow rate from 25.0 to 100.0 ml/min and slightly decreased with increasing reactant feed flow rate from 100.0 to 125.0 ml/min. It could be concluded that the reactant feed flow rate of 100.0 ml/min was an optimum reactant feed flow rate in both of the energy yield and plasma stability point of view. Therefore, the reactant feed flow rate of 50.0 and 100.0 ml/min were selected to investigate the effect of stage number.

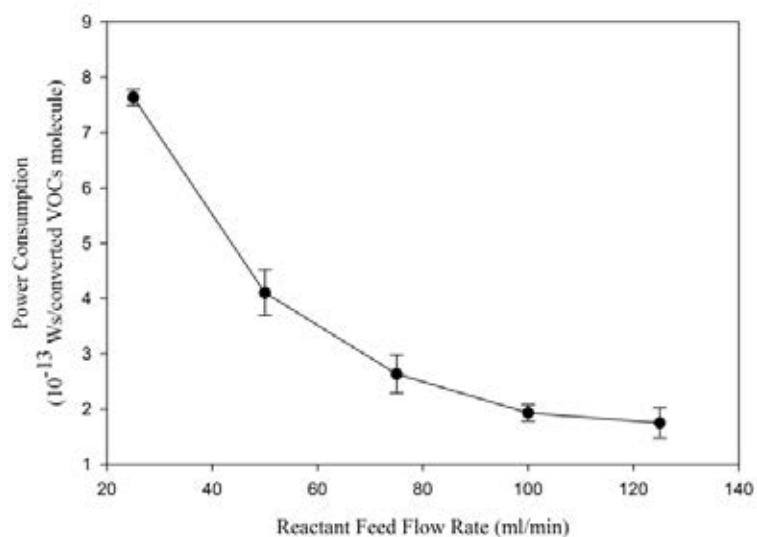


Figure 4.15 Effect of reactant feed flow rate on power consumption at applied voltage of 8 kV, input frequency of 500 Hz and initial VOCs concentration at 100 ppm.

4.5 Effect of Stage Number

As same as the effect of reactant feed flow rate, the stage number of plasma reactor also has directly affect to the residence time of reactant molecules or another product in plasma zone. Due to the instrument limitation, this research varied the stage number from single to four stage(s). The optimum operationable was kept constant at an applied voltage of 8 kV of and input frequency of 500 Hz. VOCs concentration of at 100 ppm. In order to investigate the effect of stage number for this plasma system, the reactant feed flow rate was varied at 50 and 100 ml/min. Reactant feed flow rate of 50 ml/min caused a residence time for a single, two, three and four stage(s) of 0.46, 0.92, 1.39 and 1.85 seconds respectively. In addition, it showed the half value of residence time for a reactant feed flow rate of 100 ml/min which corresponding to the residence time of 0.23, 0.46, 0.63 and 0.93 seconds for single to four stages respectively.

4.5.1 The Effect of Stage Number on Reactant Conversion

Figure 4.16 illustrate the effect of stage number on VOCs conversion. Both of reactant feed flow rate of 50.0 and 100.0 ml/min showed the same trend that the VOCs conversion increased form single to two stage(s) and maintained constant until the last stage which approximated 100 percent conversion. Aforementioned, both of reactant feed flow rate and stage number were directly impacted on the residence time of any molecules in plasma zone. Therefore, unreacted VOCs molecules would further react in the second stage providing a higher VOCs conversion. For the reactant feed flow rate of 100.0 ml/min, the VOCs conversion increased from 89.23% to 98.13% from single to two stage(s) respectively. As same as the reactant feed flow rate of 50.0 ml/min, the VOCs conversion increased from 94.84% to 97.72% from single to two stage(s). Furthermore, the reactant feed flow rate of 100.0 ml/min which could be considered as optimum reactant feed flow rate (reason would be discussed leather) also show the trend that xylene conversion would higher than toluene and xylene respectively at any studied stage number as shown in Figure. 4.17.

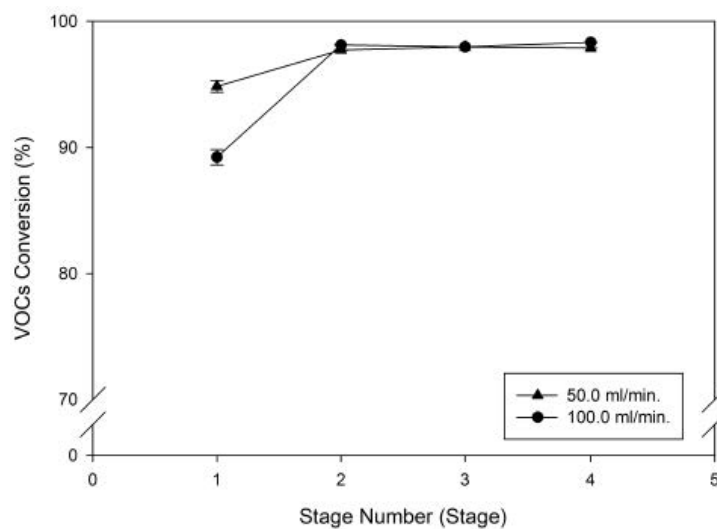


Figure 4.16 Effect of stage number on VOCs conversion at applied voltage of 8 kV, input frequency of 500 Hz, initial VOCs concentration 100 ppm, and reactant feed flow rate of 50.0 ml/min (▲) and 100.0 ml/min (●)

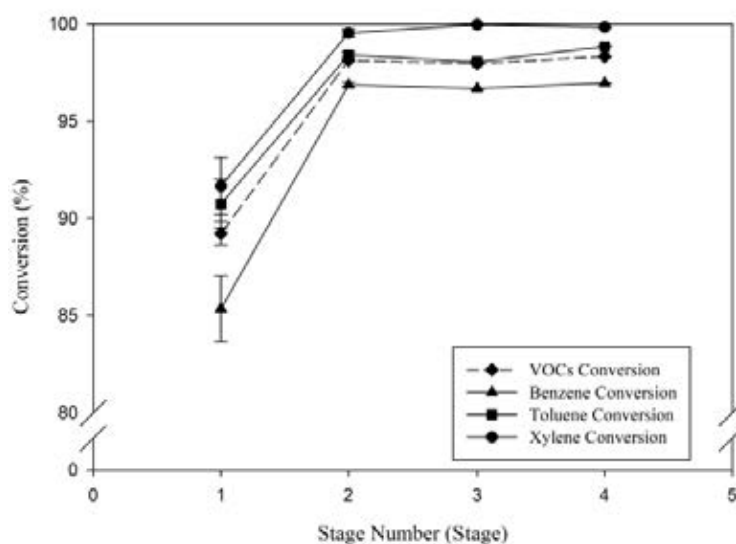


Figure 4.17 Effect of stage number on VOCs (dash line), benzene (▲), toluene (■), and xylene (●) at applied voltage of 8 kV, input frequency of 500 Hz, initial VOCs concentration 100 ppm, and reactant feed flow rate of 100.0 ml/min.

4.5.2 The Effect of Stage Number on CO and CO₂ Selectivity

Figure 4.18 showed the effect of stage number on CO and CO₂ selectivity. It could be clearly seen the CO₂ selectivity of the reactant feed flow rate at 50.0 ml/min system was higher than reactant feed flow rate at 100 ppm system at any studied stage number. In addition, the CO₂ selectivity increased dramatically from the first stage to the second stage and slightly increased with increasing to four stages. The result could be explained by the increasing of feed flow rate leading to a decreasing of residence time of VOCs or produced CO molecules in plasma zone. Therefore, the collision opportunity between CO and produced active species would be increased. For the increasing of stage number, the CO₂ selectivity would be increased especially from a single stage to two stages. Because of the residence time increased while the stage number increased, thus, there are more collision opportunity between CO and produced actives species becoming CO₂ molecules. For the third stage of reactant feed flow rate of 100.0 ml/min, CO₂ and CO selectivity was found to be 76% and 17% respectively.

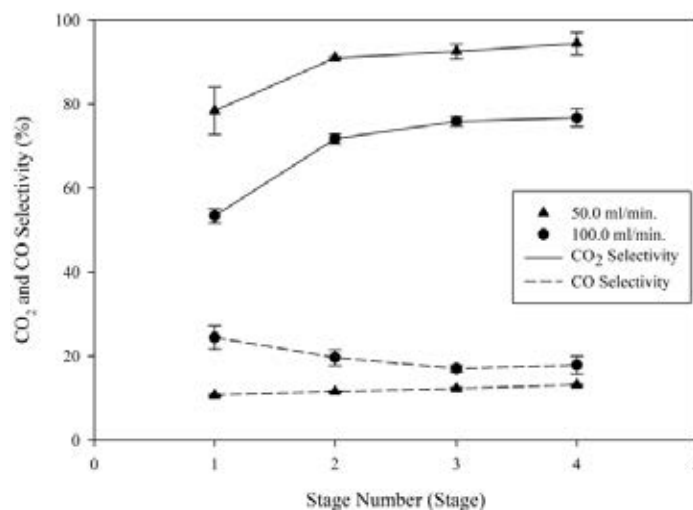


Figure 4.18 Effect of stage number on CO₂ (solid line) and CO (dash line) selectivity at applied voltage of 8 kV, input frequency of 500 Hz, initial concentration at 100 ppm and reactant feed flow rate of 50.0 ml/min (▲) and 100.0 ml/min (●).

4.5.3 The Effect of Stage Number on Power Consumption

The effect of stage number on power consumption to convert one molecule of VOCs at an optimum operationable condition was illustrated in Figure 4.19. The results showed that system would consume the more energy while the stage number was increasing at any reactant feed flow rate. For the reactant feed flow rate of 100.0 ml/min, the three stages system could be considered as the optimum operating stage number due to it consumed a low energy with provided high CO₂ selectivity.

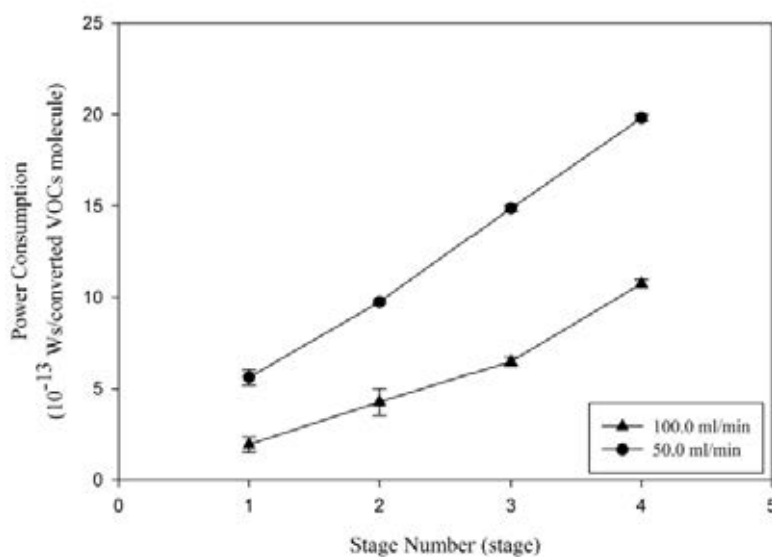


Figure 4.19 Effect of stage number on power consumption at applied voltage of 8kV, an input frequency of 500 Hz, initial VOCs concentration of 100 ppm and reactant feed flow rate of 50.0 ml/min (●) and 100.0 ml/min (▲).

4.6 Effect of Stage Number at the Same Residence Time

Residence time is another operational parameter that affected on oxidation reaction performances. In this study, residence time was fixed at 0.46 seconds corresponding to the feed flow rate of single to four stages of 50.0, 100.0, 150.0 and 200.0 ml/min. the operation conditions were fixed at an applied voltage of 8 kV, input frequency of 500 Hz and VOCs initial concentration of 100 ppm.

4.6.1 Effect of Stage Number at Residence Time on VOCs Conversion

Figure 4.20 illustrated the effect of residence time at 0.46 seconds on VOCs conversion and each of benzene, toluene and xylene conversion. the results showed that Vos conversion continuously increased with increasing of the stage number at the same total residence time. In addition, it also showed same trend that xylene conversion would higher than toluene and benzene conversion respectively. The results could be explained by the aforementioned reaction path way that the produced oxygen radicals have the longer life time after the plasma zone (Lee *et al.* 2002). Therefore, the reaction between produced oxygen radicals and VOCs molecules of the system with higher stage number could be more occurred. The results showed at VOCs conversion increased from 94.84 to 98.31% form single to two stages and it slightly increased to 98.34% at four stages.

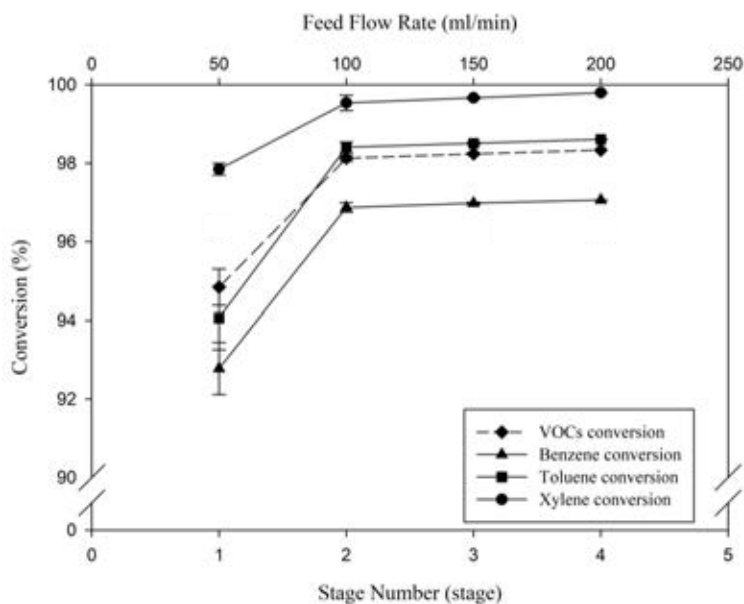


Figure 4.20 Effect of residence time at 0.46 on VOCs (dash line), benzene (\blacktriangle), toluene (\blacksquare) and xylene (\bullet) conversion at initial VOCs concentration 100 ppm, an applied voltage of 8 kV and input frequency of 500 Hz.

4.6.2 Effect of Stage Number at Residence Time CO and CO₂ Selectivity

Figure 4.21 showed the effect of residence time on CO and CO₂ selectivity. The results showed that CO₂ selectivity decreased by increasing the stage number from single to four stages at the total residence time of 0.46 seconds. On the other hand, CO selectivity increased from a single to four stages. The results could be explained by non-stable plasma formation at the first stage when feed flow rate was increased to 150.0 and 200.0 ml/min. It led to the more CO formation in the system with higher stage number. Additionally, the bond strength between carbon and oxygen atom in CO molecules would be stronger than CO₂ molecules (Urashima *et al.* 200). Therefore, the cracking possibility of CO₂ and produced CO was increased leading to higher CO selectivity.

Therefore, It could be concluded that the increasing of stage number at the same residence time could enhance the process performance by increasing VOCs conversion with higher feed flow rate but it could not enhance the product selectivity.

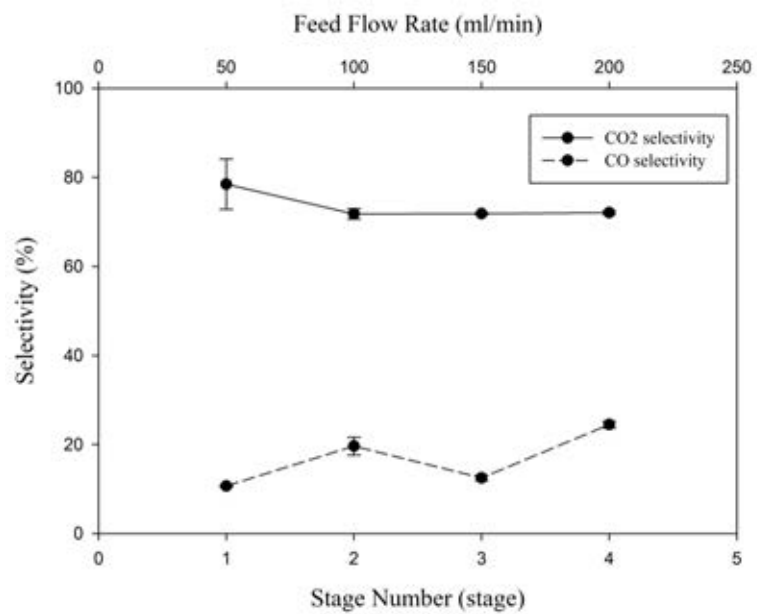


Figure 4.21 Effect of residence time at 0.46 on CO₂ (solid line) and CO (dash line) selectivity at applied voltage of 8 kV, input frequency of 500 Hz, initial concentration at 100 ppm.

CHAPTER V

CONCLUSIONS AND RECOMMENDATIONS

5.1 Conclusions

The results showed that an operation condition including applied voltage, input frequency, reactant feed flow rate and stage number played a very important role on plasma stability and also the oxidation reaction performances. The main composition in condensed product was acetic acid.

The optimum condition for a single stage corona discharge were found at an applied voltage of 8 kV, a frequency of 500 Hz and feed flow rate of 50.0 ml/min. Under these optimum conditions, the VOCs conversion and CO₂ selectivity were found to be 94.76 and 80.0%, respectively.

The increase in reactant feed flow rate from 25 to 125 ml/min corresponding to the reduction of residence time from 0.92 to 0.19 s resulted in decreases in both of VOCs conversion and CO₂ selectivity from 97.7 to 63.9% and 84.0 to 22.6%, respectively while the CO selectivity was increased from 8.2 to 62.4%. The reactant feed flow rate of 100.0 ml/min could be considered as an optimum reactant feed flow rate which provide VOCs conversion and CO₂ selectivity of 89.23 and 53.42% respectively.

The increasing in stage number from single to four stage(s) provide the residence time of 0.23, 0.46, 0.63 and 0.93 for single to four stages respectively at the reactant feed flow rate of 100.0 ml/min. The VOCs conversion was 100% at the second stage. Additionally, the three stages corona discharge could be considered as the optimum stage number. At the third stage, CO₂ and CO selectivity was found to be 75.89 and 17.04% respectively.

5.2 Recommendations

The recommendations for future work are as follows:

1. To do the corona discharge catalytic process for archive a 100 percent of carbon dioxide selectivity.

REFERENCES

- Berenjian, A., Chan, N., Malamiri, J. (2012), Volatile organic compounds removal methods: A review. American Journal of Biochemistry and Biotechnology, 8(4), 220-229.
- Chavadej, S., Kiatabolpaiboon, W., Rangsuvigit, P., Sreethawong, T. (2006), A combined multistage corona discharge and catalytic system for gaseous benzene removal. Journal of molecular catalysis A: Chemical, 263,128-136
- Chavadej, S., Saktrakool, K., Rangsanvigit, P., Lobban, L., Sreethawong, T. (2007), Oxidation of ethylene by a multistage corona discharge system in the absence and presence of Pt/TiO₂. Chemical Engineering Journal, 132, 345-353.
- Chaichanawong, J., Tanthapanichakoon, W., Charinpantikul, T., Eiad-ua, A., Sano, N., Tammon, H. (2005), High-temperature simultaneous removal of acetaldehyde and ammonia gases using corona discharge. Science and Technology of Advanced Materials, 6, 319-324.
- Chang, J. S., Lawless, P. A., Yamamoto, T. (1991), Corona discharge process. IEEE transaction on plasma science, 19(6), 1152-1166.
- Conrads, H., Schmidt, M. (2000), Plasma generation and plasma sources. IOP science, 9, 441-454.
- Czernichowski, A. (1994), Gliding arc. Applications to engineering and environment control. Pure & Appl. Chem., 66(6), 1301-1310.
- DEPARTMENT of HEALTH AND HUMAN SERVICES, Public Health Service Agency for Toxic Substances and Disease Registry. (2007) . PUBLIC HEALTH STATEMENT: Benzene. Georgia: ATSDR.
- DEPARTMENT of HEALTH AND HUMAN SERVICES, Public Health Service Agency for Toxic Substances and Disease Registry. (2000) . PUBLIC HEALTH STATEMENT: Toluene. Georgia: ATSDR.
- DEPARTMENT of HEALTH AND HUMAN SERVICES, Public Health Service Agency for Toxic Substances and Disease Registry. (2007) . PUBLIC HEALTH STATEMENT: Xylene. Georgia: ATSDR.

- Elfadly, A.M., Zeid, I.F., Yehia, F.Z., Rabie A.M., Aboualala, M.M., Park, S.E (2016), Highly selective BTX from catalytic fast pyrolysis of lignin over supported mesoporous silica. International Journal of Biological Macromolecules, 91, 278-293.
- Feng, F., Ye. L., Liu, K. (2013), Non-thermal plasma generation by using back corona discharge on catalyst. Journal of Electrostatics, 71, 179-184.
- Goldman, M. , Goldman, A. , Sigmund, R. S. (1985), The corona discharge, its properties and specific used. Pure &Appl. Chem., 57(9), 1353-1362.
- Jhonson, T., Jakobson, S., Wettervik, B., Andersson, B., Mark, A., Edlvik, F. (2015), A finite volume method for electrostatic three species negative corona discharge simulations with application to externally charged powder bells. Journal of Electrostatics, 74, 27-36.
- Kamal, M. S. , Razzak, S. A. , Hossain, M. M. (2016), Catalytic oxidation of volatile organic compounds (VOCs) - A review. Atmospheric Environment, 140, 117-134.
- Kanjanasiranont, N. , Prueksasit, T. , Morkoy, D. (2017), Inhalation exposure and health risk levels to BTEX and carbonyl compounds of traffic policeman working in the inner city of Bangkok, Thailand. Atmospheric Environment, 152, 111-120.
- Kogelschatz, U. (2003), Dielectric-barrier Discharges: Their History, Discharge Physics, and Industrial Applications. Plasma Chemistry and Plasma Processing, 23(1), 1-46.
- Lee, H., Chang, M. (2003), Abatement of Gas-phase p-Xylene via Dielectric Barrier Discharges. Plasma Chemistry and Plasma Processing, 23, 541-558.
- Lu, B. , Zhang, X. , Yu, X. , Feng, T. , Yao, S. (2006), Catalytic oxidation of benzene using DBD corona discharges. Journal of Hazardous Materials, 137, 633-637.
- Morgan, N.N. (2009), Atmospheric pressure dielectric barrier discharge chemical and biological applications. International Journal of Physical Sciences, 4(13), 885-892.
- Nojiri, K. (2015) . Dry Etching Technology for Semiconductors. Switzerland: Springer International Publishing.

- Ondarts, M., Hajji, W., Outin, J., Bejat, T., Gonze, E. (2017), Non-Thermal Plasma for indoor air treatment: Toluene degradation in a corona discharge at ppbv levels. Chemical Engineering Research and Design, 118, 194-205.
- Samanta, K., Jassal, M., Agrawal, A.K. (2006), Atmospheric pressure glow discharge plasma and its application in textile. Indian Journal of Fibre & Textile Research, 31, 83-98.
- Wan, Y., Fan, X., Zhu, T. (2011), Removal of low-concentration formaldehyde in air by DC corona discharge plasma. Chemical Engineering Journal, 171, 314-319.
- Xu, X. (2001), Dielectric barrier discharge - properties and applications. Thin Solid Films, 390, 237-242.
- Ye, Z., Zhang, Y., Li, P., Yang, L. (2008), Feasibility of destruction of gaseous benzene with dielectric barrier discharge. Journal of Hazardous Materials, 156, 356-364.
- Zhang, Z., Wang, X., Zhang, Y., Lu, S., Huang, Z., Huang, X., Wang, Y. (2015), Ambient air benzene at background sites in China's most developed coastal regions: Exposure levels, source implications and health risks. Science of the Total Environment, 511, 792-800.

APPENDICES

Appendix A Experimental data

Table A1 Effect of applied voltage on VOCs conversion and CO and CO₂ selectivity of the studied input frequency of 300, 400, 500 and 600 Hz, an initial concentration of 100 ppm, total feed flow rate of 50.0 ml/min and electrode gap distance of 10 mm

An applied voltage (kV)	Parameters	An input frequency (Hz)			
		300	400	500	600
4	VOCs Conversion (%)	91.02	93.19	90.22	69.79
	Benzene Conversion (%)	88.83	92.11	89.25	69.96
	Toluene Conversion (%)	91.03	92.96	89.5	68.37
	Xylene Conversion (%)	94	95.25	92.67	71.16
	CO selectivity (%)	13.31	12.03	14.05	27.63
	CO ₂ Selectivity (%)	83.45	75.09	77.21	67.03
	Carbon loss (%)	-2.58	1.55	-2.15	-0.77
	Current (mA)	70	60	60	60
	Power consumption ($\times 10^{-13}$)	6.78	6.19	6.38	8.2
6	VOCs Conversion (%)	97.36	97.38	91.95	92.2
	Benzene Conversion (%)	95.89	95.49	89.77	89.8
	Toluene Conversion (%)	97.69	97.61	92.18	92.76
	Xylene Conversion (%)	99.12	99.7	94.69	94.87
	CO selectivity (%)	10.23	9.49	11.94	12.62
	CO ₂ Selectivity (%)	85.6	89.28	86.62	84.4
	Carbon loss (%)	6.09	-4.24	-3.05	-2.72
	Current (mA)	130	100	80	90
	Power consumption ($\times 10^{-13}$)	6.04	6.43	6.8	7.36
8	VOCs Conversion (%)	96.31	97.83	94.76	93.92
	Benzene Conversion (%)	94.68	96.11	92.66	92.12
	Toluene Conversion (%)	96.58	98.15	94.88	94.1
	Xylene Conversion (%)	98.85	99.82	97.81	96.37
	CO selectivity (%)	10.3	7.56	10.84	10.13
	CO ₂ Selectivity (%)	86.85	93.02	79.75	84.62
	Carbon loss (%)	-3.63	-4.61	-1.54	-5.41
	Current (mA)	170	130	110	90
	Power consumption ($\times 10^{-13}$)	5.92	5.96	5.78	6.53

An applied voltage (kV)	Parameters	An input frequency (Hz)			
		300	400	500	600
10	VOCs Conversion (%)	97.96	97.77	97.68	97.79
	Benzene Conversion (%)	96.42	96.13	95.58	96.11
	Toluene Conversion (%)	98.28	97.19	97.73	98.09
	Xylene Conversion (%)	99.84	99.93	99.55	99.87
	CO selectivity (%)	9.28	10.81	8.24	9.58
	CO ₂ Selectivity (%)	93.81	88.04	90.46	88.68
	Carbon loss (%)	-5.27	-5.27	-4.82	-4.41
	Current (mA)	240	170	140	110
	Power consumption ($\times 10^{-13}$)	6.22	6.22	6.2	6.39

Table A2 Effect of input frequency on VOCs conversion and CO and CO₂ selectivity of the studied applied voltage of 4, 6, 8 and 10 kV, an initial concentration of 100 ppm, total feed flow rate of 50.0 ml/min and electrode gap distance of 10 mm.

An input frequency (Hz)	Parameters	An applied voltage (kV)			
		4	6	8	10
300	VOCs Conversion (%)	91.02	97.36	96.31	97.96
	Benzene Conversion (%)	88.83	95.89	94.68	96.42
	Toluene Conversion (%)	91.03	97.69	96.58	98.28
	Xylene Conversion (%)	94	99.12	98.85	99.84
	CO selectivity (%)	13.31	10.23	10.3	9.28
	CO ₂ Selectivity (%)	83.45	85.6	86.85	93.81
	Carbon loss (%)	-2.58	6.09	-3.63	-5.27
	Current (mA)	70	130	170	240
	Power consumption ($\times 10^{-13}$)	6.78	6.04	5.92	6.22
400	VOCs Conversion (%)	93.19	97.38	97.83	97.77
	Benzene Conversion (%)	92.11	95.49	96.11	96.13
	Toluene Conversion (%)	92.96	97.61	98.15	97.19
	Xylene Conversion (%)	95.25	99.7	99.82	99.93
	CO selectivity (%)	12.03	9.49	7.56	10.81
	CO ₂ Selectivity (%)	75.09	89.28	93.02	88.04
	Carbon loss (%)	1.55	-4.24	-4.61	-5.27
	Current (mA)	60	100	130	170
	Power consumption ($\times 10^{-13}$)	6.19	6.43	5.96	6.22

An input frequency (Hz)	Parameters	An applied voltage (kV)			
		4	6	8	10
500	VOCs Conversion (%)	90.22	91.95	94.76	97.68
	Benzene Conversion (%)	89.25	89.77	92.66	95.58
	Toluene Conversion (%)	89.5	92.18	94.88	97.73
	Xylene Conversion (%)	92.67	94.69	97.81	99.55
	CO selectivity (%)	14.05	11.94	10.84	8.24
	CO ₂ Selectivity (%)	77.21	86.62	79.75	90.46
	Carbon loss (%)	-2.15	-3.05	-1.54	-4.82
	Current (mA)	60	80	110	140
	Power consumption ($\times 10^{-13}$)	6.38	6.8	5.78	6.2
600	VOCs Conversion (%)	69.79	92.2	93.92	97.79
	Benzene Conversion (%)	69.96	89.8	92.12	96.11
	Toluene Conversion (%)	68.37	92.76	94.1	98.09
	Xylene Conversion (%)	71.16	94.87	96.37	99.87
	CO selectivity (%)	27.63	12.62	10.13	9.58
	CO ₂ Selectivity (%)	67.03	84.4	84.62	88.68
	Carbon loss (%)	-0.77	-2.72	-5.41	-4.41
	Current (mA)	60	90	90	110
	Power consumption ($\times 10^{-13}$)	8.2	7.36	6.53	6.39

Table A3 Effect of reactant feed flow rate on VOCs conversion and CO and CO₂ selectivity at applied voltage of 8 kV, input frequency of 500 Hz, an initial concentration of 100 ppm and electrode gap distance of 10 mm.

Parameters	Reactant feed flow rate (ml/min)				
	25	50	75	100	125
VOCs Conversion (%)	97.21	97.7	97.54	89.23	67.93
Benzene Conversion (%)	95.42	95.97	96.23	85.35	71.48
Toluene Conversion (%)	97.47	98.01	97.85	90.76	74.87
Xylene Conversion (%)	99.38	99.82	98.94	91.67	55.96
CO selectivity (%)	17.69	8.22	8.92	24.4	61.83
CO ₂ Selectivity (%)	68.93	84	64.55	53.42	22.07
Carbon loss (%)	5.34	-1.22	4.64	7.76	-2.69
Current (mA)	110	110	100	90	90
Power consumption ($\times 10^{-13}$)	7.64	4.11	2.64	1.93	1.75

Table A4 Effect of stage number rate on VOCs conversion and CO and CO₂ selectivity at applied voltage of 8 kV, input frequency of 500 Hz, an initial concentration of 100 ppm, electrode gap distance of 10 mm and reactant feed flow rate of 50.0 and 100.0 ml/min.

Reactant feed flow rate (ml/min)	Parameters	Stage number (stage)			
		1	2	3	4
50	VOCs Conversion (%)	94.84	97.72	97.97	97.88
	Benzene Conversion (%)	92.78	96.21	96.5	96.32
	Toluene Conversion (%)	94.97	97.9	98.25	98.16
	Xylene Conversion (%)	97.85	99.81	99.9	99.92
	CO selectivity (%)	10.66	11.54	12.28	13.2
	CO ₂ Selectivity (%)	78.43	90.99	92.52	94.4
	Carbon loss (%)	0.06	-9.85	-9.65	-10.23
	Current (mA)	110	220	330	440
	Power consumption ($\times 10^{-13}$)	5.85	10.15	15.5	20.64
100	VOCs Conversion (%)	89.23	98.13	97.98	98.33
	Benzene Conversion (%)	85.35	96.87	96.68	96.96
	Toluene Conversion (%)	90.76	98.41	98.06	98.63
	Xylene Conversion (%)	91.67	99.54	99.97	99.84
	CO selectivity (%)	24.4	19.63	17.04	17.88
	CO ₂ Selectivity (%)	53.42	71.77	75.89	76.76
	Carbon loss (%)	7.76	0.78	-11.59	-2.96
	Current (mA)	110	200	330	440
	Power consumption ($\times 10^{-13}$)	2.02	4.27	6.48	10.75

Table B1 Products information from GC-MS analysis

Name	Formula	Retention time (s)	Area	Height
Formic acid	CH ₂ O ₂	307.2	2087064	6.1349
Acetic acid	C ₂ H ₄ O ₂	319.6	15928690	46.822
Ethanol, 2-nitro-, propionate (ester)	C ₅ H ₉ NO ₄	342.1	104248	0.30644
2-Propenoic acid	C ₃ H ₄ O ₂	344.5	232668	0.68392
Acetic anhydride	C ₄ H ₆ O ₃	364.7	1051713	3.0915
CH ₃ C(O)CH ₂ CH ₂ OH	C ₄ H ₈ O ₂	470.65	548540	1.6124
Furfural	C ₅ H ₄ O ₂	508.6	143486	0.42177
2-Cyclopenten-1-one	C ₅ H ₆ O	526.3	309961	0.91112
Cyclopent-4-ene-1,3-dione	C ₅ H ₄ O ₂	660.15	439221	1.2911
4-Cyclopentene-1,3-dione	C ₅ H ₄ O ₂	672.9	639934	1.8811
3,4 Epoxytetrahydrothiophene-1,1-dioxide	C ₄ H ₆ O ₃ S	684.05	66955	0.19681
Phenol	C ₆ H ₆ O	688.9	358795	1.0547
p-Benzoquinone	C ₆ H ₄ O ₂	706.5	1073177	3.1546
Benzaldehyde	C ₇ H ₆ O	710.75	3819624	11.228
2(5H)-Furanone	C ₄ H ₄ O ₂	746.75	303429	0.89192
2H-Pyran-2-one	C ₅ H ₄ O ₂	820.4	176778	0.51964
Benzyl alcohol	C ₇ H ₈ O	831.4	2035866	5.9844
1,4-Cyclohex-2-enedione	C ₆ H ₆ O ₂	931.15	120936	0.35549
3-Methylbenzyl alcohol	C ₈ H ₁₀ O	1000.55	650300	1.9115
Isophthalaldehyde	C ₈ H ₆ O ₂	1314.4	143485	0.42177

CURRICULUM VITAE

Name: Mr. Nitikorn Ditthawat

Date of Birth: November 12, 1993

Nationality: Thai

University Education:

2012–2016 Bachelor Degree of Petrochemical and Polymeric Materials, Faculty of Engineering and Industrial Technology, Silpakorn University, Nakorn Phathom, Thailand.

Proceeding:

1. Ditthawat, N.; and Chavadej, S. (2018, April 22nd), Removal of Mixed VOCs by a multistage corona discharge system. Proceedings of the 9th Research Symposium on Petrochemical and Materials Technology and the 24th PPC Symposium on Petroleum, Petrochemicals, and Polymers, Bangkok, Thailand.

Presentations:

2. Ditthawat, N.; and Chavadej, S. (2018, April 22nd), Removal of Mixed VOCs by a multistage corona discharge system. Proceedings of the 9th Research Symposium on Petrochemical and Materials Technology and the 24th PPC Symposium on Petroleum, Petrochemicals, and Polymers, Bangkok, Thailand.